Cellulose (2020) 27:799–823
https://doi.org/10.1007/s10570-019-02799-x

ORIGINAL RESEARCH

The effect of Ru/C and $MgCl_2$ on the cleavage of inter- and intra-molecular linkages during cornstalk hydrolysis residue valorization

Wei Lv · Yuhe Liao · Yuting Zhu · Jing Liu · Changhui Zhu · Chenguang Wang · Ying Xu · Qi Zhang · Guanyi Chen · Longlong Ma

Received: 14 March 2019 / Accepted: 17 October 2019 / Published online: 15 November 2019

Abstract The cleavage of linkages of lignocellulose is important for its valorization. The linkage cleavage of cornstalk hydrolysis residue was investigated over catalysts (Ru/C + $MgCl_2$) in EtOAc/H_2O solvents. The results show that almost hydrogen bonds, C–C bonds, ether and ester bonds in the matrix of lignin and cellulose were broken, accompanying 80.6% of lignin and 98.5% of cellulose conversion, and obtaining 37.5% of aromatic monomers and 28.8% of lignin oligomers. In the reaction system, biphasic EtOAc/H_2O solvents exhibited an effect on cleaving the intermolecular linkages between lignin and cellulose. $MgCl_2$ showed limited abilities of breaking the α-O-4 and β-O-4 linkages in lignin and limited β-1, 4-glycosidic and hydrogen bonds in cellulose were cleaved over Ru/C catalyst. The cleavage of C–O linkages (α-O-4, β-O-4, 4-O-5) and C–C bonds (α-β, β-5) in lignin were mainly dependent on Ru/C catalyst. Much C–O and the stubborn C–C linkages of β-5, β-1 and 5-5 were significantly disrupted by the synergistic effect between $MgCl_2$ and Ru/C. However, $MgCl_2$ exhibited great contribution to breakage of β-1, 4-glycosidic linkage, hydrogen bonds and sugar ring of cellulose. The linkage of β-1, 4-glycosidic, hydrogen bonds and

Electronic supplementary material The online version of this article (https://doi.org/10.1007/s10570-019-02799-x) contains supplementary material, which is available to authorized users.

W. Lv · Y. Zhu · J. Liu · C. Zhu · C. Wang (✉) · Y. Xu · Q. Zhang · L. Ma (✉)
CAS Key Laboratory of Renewable Energy, Guangdong Provincial Key Laboratory of New and Renewable Energy Research and Development, Guangzhou Institute of Energy Conversion, Chinese Academy of Sciences, No.2 Nengyuan Rd., Tianhe District, Guangzhou 510640, China
e-mail: wangcg@ms.giec.ac.cn

L. Ma
e-mail: mall@ms.giec.ac.cn

W. Lv · G. Chen · L. Ma
School of Environmental Science and Engineering, Tianjin University, No.92 Weijin Rd., Nankai District, Tianjin 300000, People's Republic of China

Y. Liao
Center for Surface Chemistry and Catalysis, Katholieke Universiteit Leuven, Celestijnenlaan 200F, 3001 Heverlee, Belgium

W. Lv
Key Laboratory of Biomass Energy and Material, Jiangsu Province, No. 16 5th Suojin Village, Xuanwu District, Nanjing 210018, China

C–C in C5/C6 sugars were significantly broken. The increased yield of products was evidently due to the synergistic effect of Ru/C combined with $MgCl_2$.

Keywords Cleavage of linkage · Biphasic EtOAc/H_2O solvents · Ru/C · $MgCl_2$ · Cornstalk hydrolysis residue (CHR) · Valorization

Introduction

The significant sustainability and economic features of biomass valorization attract more and more attention (Chheda et al. 2007; Roman-Leshkov et al. 2007; Somerville et al. 2010). Cellulose and hemicellulose can be transformed to added-value chemicals and fuels, such as, ethanol, soap, pulp, hydroxymethylfurfural (HMF), γ-valerolactone (GVL) and alkanes (Hanson et al. 2009; Zakzeski et al. 2010; Xu et al. 2014). Lignin-derived monomers are being utilized in aromatic components, resins, platform aromatics and other chemicals. Di- and oligomers are relevant in certain applications like producing polyurethanes and polyesters (Ragauskas et al. 2014; Gandini 2011; Van den Bosch et al. 2015a).

To improve the biorefinery economy, conversion of all fractions of lignocellulose into platform chemicals or materials is goal. For example, some work focused on introducing 'lignin-first' disassembly processing of raw lignocellulose with various solvents with/without external H_2 over different catalysts(Ferrini and Rinaldi 2014; Van den Bosch et al. 2015b; Shuai et al. 2016; Galkin and Samec 2014, 2016). Sels et al. reported that 90% of lignin was obtained as a ''lignin oil'' in methanol at elevated temperature over Ru/C under a mild H_2-pressure, comprising mainly phenolic monomers, dimers, and small oligomers (Van den Bosch et al. 2015b). Luterbacher et al. published a 75.4 wt% of lignin could be extracted from corn stover using H_2SO_4/H_2O/GVL system to yield lignin-derived monomers corresponding to 38% of the carbon in the original lignin (Luterbacher et al. 2015). Rinaldi et al. described that most of lignin in plant biomass can be effectively depolymerized into non-pyrolytic lignin bio-oil through *iso*-propanol hydrogen transfer reaction in the presence of Raney Ni, next to a solid carbohydrate pulp (Ferrini and Rinaldi 2014). Results also show that lignin was disassembled from various lignocellulose materials and simultaneously left a very high proportion of carbohydrates in the pulp. These pulps towards added-value chemicals were demonstrated by their conversion to polyols/sugars in further processing (Liu et al. 2015; Geboers et al. 2011b; Ruppert et al. 2012). Li et al. recently published that formaldehyde as a stabilizer facilitated soluble lignin fraction production during biomass pretreatment, high yields of guaiacyl and syringyl monomers were obtained from the isolated lignin. Meanwhile, by depolymerizing cellulose, hemicelluloses, and lignin separately, monomer yields were between 76 and 90 C-mol% for these three major biomass fractions (Shuai et al. 2016). In all of these biorefinery strategies, monomers were considered as the "star" platform chemicals for further upgrading to produce high-value fuel via hydrogenolysis or/and hydrodeoxygenation technologies (Zhao et al. 2009; Jiang et al. 2016a). Thus, the efficient disassembly and separation of matrix components directly from lignocellulose to monomers with high yield is crucial for added-value biofuel production. Although these technologies show promise for future biorefineries, the current biorefinery still uses cellulose first, leaving lignin as a residue. (cellulose is converted into chemicals first, and leave lignin as a residue). Especially, hydrolysis is the main industrial route to valorize lignocellulose into chemicals like ethanol. Although the products are a mixture of phenolics, they can be transformed into bio-fuels or bulk chemicals like adipic acid via chemo- or bio-catalysis (Payne et al. 2013; Resch et al. 2013). To valorize this residue (rich in lignin) is also important for improving biorefinery economy (De Bruyn et al. 2016). As we known, lignin connects cellulose or/and hemicellulose by chemical bonds to form LCC in plant cell wall or pulp lignin. For instance, Henry I. Bolker measured lignin carbohydrate bond with infrared spectroscopy, showing that an acetal or hemi-acetal bond existed between carbonyl groups of lignin and the hydroxyl groups of some portion of the holocellulose (Bolker 1963). With the development of analytic techniques, several kinds of LCC linkages (i.e., ether type (benzyl ether or/and acetal), ester type and ketal type) were confirmed between C_6 position of glucose units in cellulose and α-C of lignin side chain with ^{13}C isotopic tracer technique in ^{13}C NMR/HSQC (Miyagawa et al. 2013; Huber et al. 2006; Dornath et al. 2015). Those linkage bonds (intermolecular and intramolecular,

such as ether bond, ester bond, hydrogen bond, C–C and C–O bonds) between lignin and the other components of lignocellulose and intramolecular linkage of lignin (β-O-4, α-O-4, β-β, β-5, etc.) impede the deconstruction of cross-linked unit building blocks (Ragauskas et al. 2014; Jiang et al. 2016a). Therefore, understanding the cleavage behavior of inter- and intramolecular linkages rules is very important.

In terms of the scission of inter- and intramolecular linkages of lignin, numerous researches based on lignin model compounds were published. C–O bonds of aryl ethers could be effectively fractured with/without external H_2 over Ni-based catalysts (Molinari et al. 2014; Sergeev et al. 2012; Kelley et al. 2012; He et al. 2012; Sturgeon et al. 2014), while noble metals can effectively break C–C bonds in β-O-4 linkages (vom Stein et al. 2015). However, the linkage cleavage of these simplified model compounds could hardly be transferred to real lignocellulose. In this context, a few group's attention was drawn to investigate inter- and intramolecular linkage cleavage mechanisms in specific biorefinery strategies. Luterbacher et al. investigated the structure of lignin fraction obtained from corn stover processed in H_2SO_4/H_2O/GVL system to produce monomers (Luterbacher et al. 2015). Hu et al. investigated the cleavage behavior of inter- and intramolecular linkages in corncob residue for producing monophenols in Na_2CO_3–H_2O–THF system (Jiang et al. 2016a). In their work, H_2O may be responsible for the cleavage of relatively weak inter- and intra-bonds in corncob residue, whereas almost all intermolecular linkages of ether, ester and hydrogen bonds between lignin and cellulose were broken by Na_2CO_3 at 140 °C; Intramolecular linkages were partially destroyed at 300 °C with 26.9 wt% yield of monophenols. The product structures indicated that Na_2CO_3 promoted to break the C–O bond in β-O-4 linkage and C_α–C_β bond in the aliphatic side-chain of lignin to obtain aryl aldehyde, as well as the cleavage of C_{Ar}–C_α bond. Jastrzebski. R. et al. worked out a tandem catalysis strategy for ether linkage cleavage of lignin and its model compounds, involving ether hydrolysis by water-tolerant Lewis acids followed by aldehyde decarbonylation by Rh complex. Meanwhile, this strategy was conducted on softwood, hardwood, and herbaceous dioxasolv lignins degradation, as well as poplar sawdust, to give the anticipated decarbonylation products whose selectivity can be tuned by variation of the Lewis-acid strength and lignin source (Jastrzebski et al. 2016). Barta et al. described a new strategy that diols was used as stabilizer agent to capture unstable compounds derived from lignin, coupled with catalytic hydrogenation or decarbonylation process can gain high aromatics yield (Deuss et al. 2015). In order to execute in-depth catalysis studies and understand a detailed mechanism of lignin catalytic valorization, they synthesized a new class of (β-O-4)–(β-5) advanced di-linkages model compounds to investigate the reactivity of linkage bonds scission. They documented a detailed understanding of HOTf acid-catalyzed cleavage of various types of lignin linkages in combined with stabilizer agent (ethylene glycol) (Lahive et al. 2016). Thus, it is favorable for optimize lignocellulose depolymerization strategy by understanding the cleavage reactivity of the linkages in lignocellulose.

Based on our previous work (Lv et al. 2017), Cornstalk hydrolysis residue (CHR) was degraded over Ru/C combined with $MgCl_2$ under biphasic EtOAc/H_2O solvent to selectively produce aromatics with a yield of 30.4% without external H_2, accompanying nearly all carbohydrate liquefied. However, the cleavage mechanism of inter-and intramolecular linkages among the main components (lignin and cellulose) is not clear. In this paper we give an insight into the cleavage behavior of inter- and intramolecular linkages between cellulose and lignin of lignin/cellulose in CHR in biphasic EtOAc/H_2O solvent system over Ru/C cooperated with $MgCl_2$.

Experimental section

Materials

Ethyl acetate (EtOAc, 99%), acetic acid (99%) and $(NH_4)_2CO_3$ were analytical grade and purchased from Guangzhou Maolin Fine Chemical Co., Ltd. (Guangzhou, China). 5 wt% Ru/C was provided from Shanghai Aladdin biochemical technology co., LTD (Shanghai, China) and used as received. CHR is the hydrolyzed residue of cornstalk chips (particle size about 40 mesh) over 8.0 wt% sulfuric acid at 180 °C for 2 h at the 316L stainless steel hydrolysis reactor (from Yingkou Pilot, Liaoning China). The CHR was collected and washed with distilled water to the filtrate at pH about 7.0, then dried at 105 °C. The component analysis showed that it contains 60.98% lignin, 26.21%

cellulose, 0.52% hemicellulose, 2.15% moisture, 5.67% extraction and 3.38% ash. Elemental analysis demonstrated that it is composed of 58.73% C, 6.26% H, 0.31% N, 0.12% S and 36.28% O.

Typical process for CHR depolymerization

2.0 g CHR, 0.5 g 5 wt% Ru/C (or/and 1.0 g $MgCl_2$) and 50 mL reaction medium (40 mL of EtOAc and 10 mL of H_2O) were put into a 100 mL stainless autoclave (316L stainless, made by Anhui Kemi Machinery Technology Co., Ltd.) equipped with a mechanical stirring. After the air displacement by N_2 for three times, the reactor was heated to 200 °C and then kept for 5 h with continuous stirring at 500 rpm. After that, the reactor was cooled in an iced-water bath.

Product separation

The separation process for the reaction products was showed in Scheme 1. Gases were collected after the stainless autoclave cooled. The products were filtrated and divided to two parts (solid fraction and liquid products). The solid fraction (catalyst and depolymerization residue solid (DRS)) was washed with EtOAc (5 mL per time, three times) and H_2O (5 mL per time, three times), respectively, followed by filtration. The filtrate was mixed with liquid mixture (1). Then the liquid product was neutralized with $(NH_4)_2CO_3$ until the pH value of liquid to neutral. The liquid mixture (2) were separated to H_2O phase (bottom) and organic phase (upper). The DSR and catalyst were dried at 105 °C overnight. The aqueous phase mainly contains oligosaccharides, monomers, un-degraded lignin, and organic phase included volatile products and non-volatile products. The volatiles were the aromatic components that can be detected by GC–MS, while the non-volatiles were the residual fractions after the solvents and low boiling point of substances were removed from organic phase product through vacuum-rotary evaporation at 45 °C.

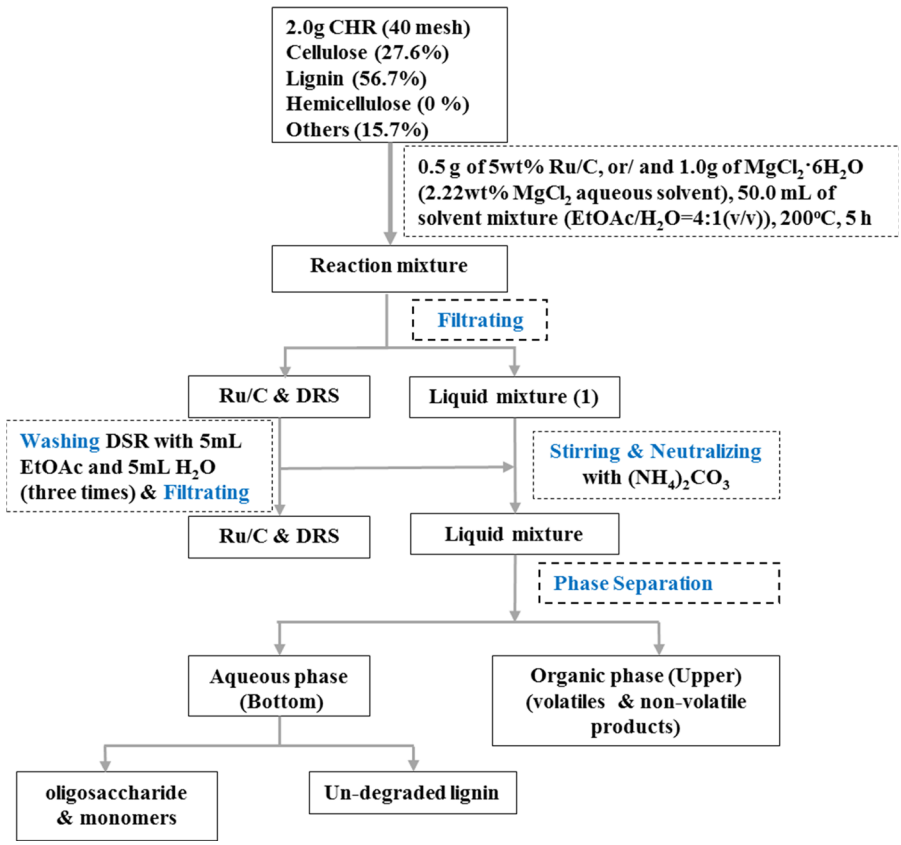

Scheme 1 Procedure for products separation

Determine the components of CHR and DSR

The components of CHR and DSR were measured according to NREL K-lignin analysis(Sluiter et al. 2008; Lv et al. 2017). CHR and DRS were characterized by Fourier translation infrared spectroscopy (FT-IR). They were analyzed on a TENSOR27 FT-IR spectrometer in the range of 4000–400 cm^{-1}, scan times is 32. Before the analysis, CHR and DSR were dried at 105 °C overnight, then ground with KBr and pressed into a wafer.

Analysis and measurement of the products

The volatile products in organic phase were detected by GC–MS (Agilent 7890A-5975C) equipped with a Pxi-17Sil MS Cap. Column (30 m × 0.25 mm × 0.25 μm) and compositions were identified according to the NIST MS library. The oven temperature was programmed as 40 °C hold 5 min, and then ramped up to 300 °C with 5.2 °C/min and hold for another 4 min. The quantitative analysis of the composition was conducted on an Agilent 7890 GC with a flame ionization detector (FID). Acetophenone was used as internal standard at the same capillary column and temperature program as the GC–MS analysis.

The LC–MS was empolyed to analyze water soluble fractions on a quadrupole-time chromatography–mass spectrometry (LC–MS, Agilent, USA) equipped with HiP Sampler, Binary Pump and triple-quadrupole Mass Spectrometer (TOF/Q-TOF).

The molecular weight of non-volatile fraction in organic phase were analyzed by gel permeation chromatography (GPC) (Algient 1260 HPLC) with a differential refraction detector (RID). The average molecular weight of the sample was measured according to the external standard method with narrow polystyrene as the standard compound. The conversion of CHR and the yield of DRS were calculated by the weight comparison between the recovered and the feedstock as shown in Eqs. (1) and (2). The conversion of lignin and cellulose were measured by the weight comparison between the recovered and the original lignin and cellulose as shown in Eqs. (3) and (4), respectively. The yield of linear alcohols/esters, aromatics and non-aromatic cyclic compounds was measured according to Eqs. (5), (6) and (7) based on the GC results, respectively. As the Scheme 1 shown, the liquid products were separated into aqueous phase and organic phase. Organic phase comprises of linear alcohols/esters, aromatics and non-aromatic cyclic compounds and non-volatile fraction. Therefore, the yield of water soluble fraction and non-volatile fraction were calculated by the weight subtraction method [Eqs. (8) and (9)].

$$\text{Conversion of CHR}(\%) = [(W_a - W_r)/W_a] \times 100\% \quad (1)$$

$$\text{Yield of DRS}\ (\%) = (W_r/W_a) \times 100\% \quad (2)$$

$$\text{Conversion of lignin}\ (\%) = \left[\left(L_0 \times W_a - L_1 \times W_r\right)/\left(L_0 \times W_a\right)\right] \times 100\% \quad (3)$$

$$\text{Conversion of cellulose}\ (\%) = [(C_0 \times Wa - C_1 \times W_r)/(C_0 \times W_a)] \times 100\% \quad (4)$$

$$\text{Yield of linear alcohols/esters}\ (\%) = [W_{aa}/(C_0 \times Wa)] \times 100\% \quad (5)$$

$$\text{Yield of aromatics}\ (\%) = [W_{ac}/(L_0 \times W_a)] \times 100\% \quad (6)$$

$$\text{Yield of non - aromatic cyclics}\ (\%) = [W_{nac}/(C_0 \times Wa)] \times 100\% \quad (7)$$

$$\text{Yield of non - volatile products}\ (\%) = \left[W_{nvp}/(L_0 \times W_a)\right] \times 100\% \quad (8)$$

$$\text{The mass of non - volatile water soluble fractions}\ (g) = W_{wsp} \quad (9)$$

W_a: the weight of CHR feedstock; Wr: the weight of DRS. W_{aa}: the weight of linear alcohols/esters. W_{ac}: the weight of volatile aromatic compounds. W_{nac}: the weight of non-aromatic cyclic compounds. W_{nvp}: the weight of EtOAc phase after removed all solvents and volatile substances. W_{wsp}: the weight of water soluble phase after removed water and volatile substances; L_0: the content of lignin in CHR feedstock (L_0 = 60.98%); L_1: the content of lignin in DRS; C_0: the content of cellulose in CHR feedstock (C_0 = 26.21%); C_1: the content of cellulose in DSR. The content of linear alcohols/esters, non-aromatic cyclic compounds and volatile aromatic compounds were measured by GC

with the same capillary column (Pxi-17Sil MS Cap., 30 m × 0.25 mm × 0.25 μm)) and temperature program as the GC–MS analysis. Acetophenone was employed as internal standard compound. The weight of others and water-soluble phase were both obtained by weight after the solvents and volatile substances removed. In addition, L_0, L_1, C_0 and C_1 were determined following standard NREL procedures (Sluiter et al. 2008).

^{1}H and ^{1}H–^{13}C HSQC NMR analysis of non-volatile fraction, CHR and DRS

To investigate the depolymerization performance and the evolution of structure on the CHR and DRS, NMR spectra of CHR, DRS and non-volatile fractions were measured by using a Bruker Avance III 400 MHz spectrometer. Both CHR (100 mg) and DRS (100 mg) were dissolved in dimethylsulfoxide-d6 ([D6] DMSO) (1.0 mL), and about 50 mg non-volatile fraction was dissolved in 0.5 mL [D6] DMSO. For the HSQC analysis, the collecting and processing parameters were listed as follows: number of scans, 84; receiver gain, 203; acquisition time, 0.2129/0.0636 s; relaxation delay, 2.0 s; pulse width, 10 s; spectrometer frequency, 400.15/100.61 MHz; and spectral width, 4807.8/20124.9 Hz (Huang et al. 2014; Zhang et al. 2015). The MestReNova software was used to process the data.

Analysis of DSR

CHR and DSR powder X-ray diffraction (XRD) patterns were measured by an X-ray diffractometer (X'Pert Pro MPD, Philip) with Cu Kα radiation (λ = 0.15418 nm) operated at 40 kV and 100 mA. The 2θ angles were scanned from 5° to 80°.

Results and discussion

Effect of EtOAc/H_2O on the cleavage of intermolecular linkages between lignin and cellulose

The developing analytic techniques have found and confirmed a large amount of intermolecular linkages of LCC in plant cell wall (lignin connects cellulose or/and hemicellulose by chemical bonds) and intramolecular linkages of lignin and cellulose or hemicellulose matrix (Xie et al. 2000; Min et al. 2014; Miyagawa et al. 2013). Examples would be the intramolecular bonds of cellulose are hydrogen and β-1,4-glucosidic bonds (Scheme 2A) and lignin's are C–O and C–C (β-O-4, α-O-4, β-β, β-5, etc.) (Scheme 2C). The intermolecular linkage between lignin and cellulose are ester, ether and ketal chemical bonds. They confirmed the C6 position of glucose units in cellulose were linked to α-C of lignin side chain and carbonyl groups of lignin linked to hydroxyl groups of some portion of the holocellulose (Scheme 2D).

As we known, solvents receive growing attention due to their important role in lignin dissolution, such as H_2O, methanol, ethanol, isopropanol and EtOAc (Marcus 1993; Shuai and Luterbacher 2016) were widely used in lignocellulose extraction and valorization (Ferrini and Rinaldi 2014; Galkin et al. 2015; de Clippel et al. 2012). Generally, H_2O, as a nucleophile reagent with high hydrogen bond accept ability, was not noly essential to reacting with the linkages (such as ether and ester bonds) between lignin and cellulose, but also had effect on disrupting the intermolecular hydrogen bonds between lignin and cellulose (Ferrini and Rinaldi 2014; Jiang et al. 2016a). When the EtOAc/H_2O volume ratio was 0:10, 21.4% of cellulose was converted and degradated products were collected to aqueous phase (Fig. 1), showing the strongest typical vibration adsorption of cellulose (1374, 1057 and 896 cm^{-1}, Fig.S1) in FT-IR spectrum of aqueous phase product. However, the conversion of lignin in pure H_2O was limited (∼ 5.6%). EtOAc, the polarity is lower than H_2O, although presents good extraction ability of lignin fragments, about 11.0% of lignin and ∼ 5.2% of cellulose in the matrix were dissolved in pure EtOAc system (Fig. 1 and Fig. S1).

Compared to pure H_2O and pure EtOAc, EtOAc/H_2O co-solvents showed much higher CHR dissolution ability and selectivity to lignin component (Fig. 1 and S1), ascribing to the strong hydrogen bond between organic solvents and H_2O that could be beneficial to the cleavage of linkages between lignin and cellulose (Zhang et al. 2018). The volume ratio of EtOAc/H_2O, with different co-solvents properties, displayed distinct effect on lignin and cellulose dissolution. For example, the dissolution of lignin increased and the aromatic ring characteristic vibration strengthened with the EtOAc/H_2O volume ratio

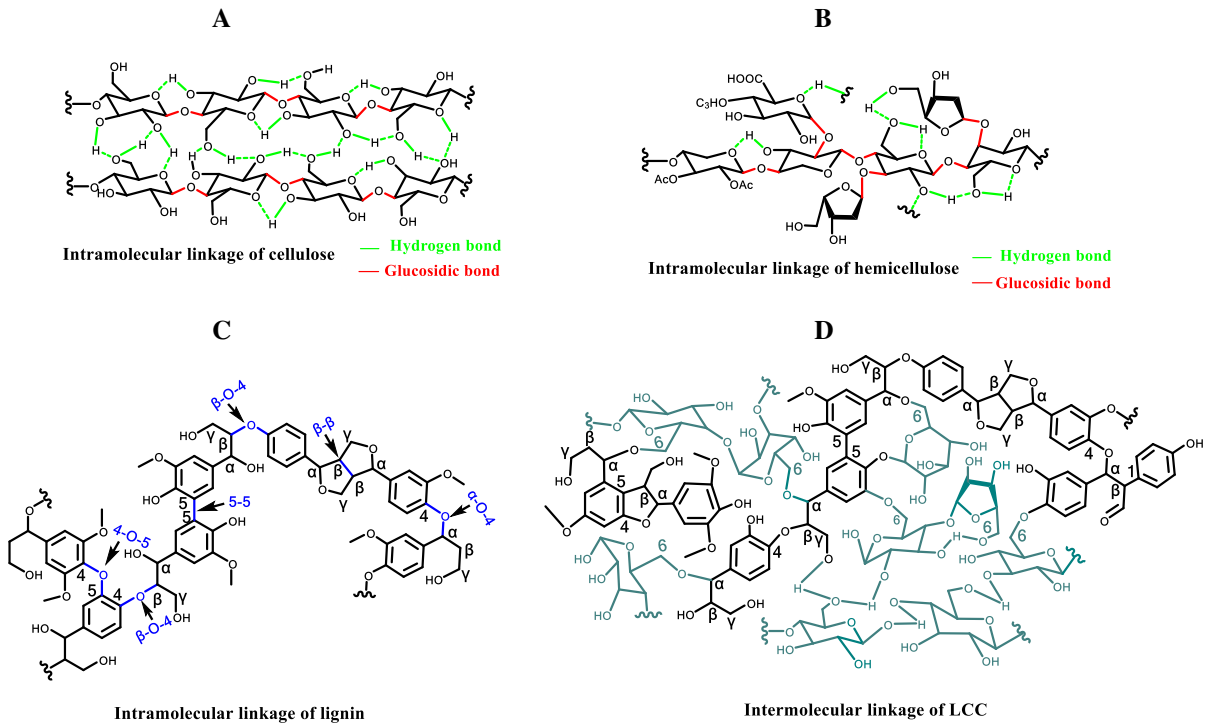

Scheme 2 The presentation of intra-/intermolecular linkage of lignocellulose (Huber et al. 2006; Dornath et al. 2015; Kadokawa et al. 2001; Min et al. 2014; Miyagawa et al. 2013; Oh et al. 2005)

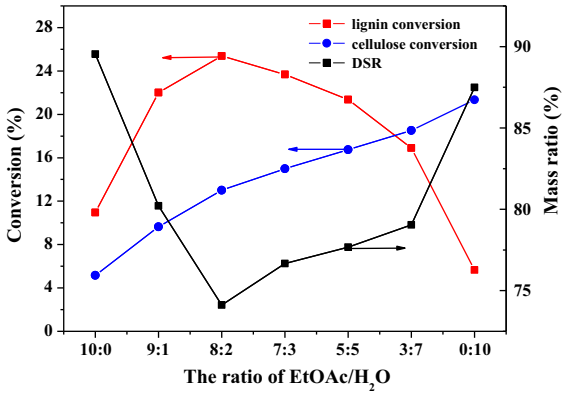

Fig. 1 Effect of the solvent volume ratio on lignin and cellulose conversion and the mass of DSR. Reaction condition: CHR feedstock (2.0 g, 40 mesh), solvent mixture (50.0 mL, EtOAc/H_2O = 10:0, 9:1, 8:2, 7:3, 5:5, 3:7, 0:10 (v/v)), 200 °C, 5 h

decreasing from 10:0 to 8:2. However, opposite trend was given with volume ratio from 8:2 to 0:10 further decreased (Fig. 1 and Fig. S2). The highest lignin and CHR conversion and the lowest M_w, M_n and D values of fragments were obtained at the point of 8:2 (Fig. 1 and Table 1). It is mainly due to the property of biphasic EtOAc/H_2O (8:2, v/v) which provided a suitable EtOAc hydrolytic rate and adjusted the polarity of mixed solvents for CHR dissolution and

Table 1 Average molecular weight of depolymerization products in different solvent volume ratio of EtOAc/H_2O without catalyst

Solvent volume ratio (v/v)	M_n[a]	M_w[a]	M_z[a]	D[a]
10:0	383	3184	242,744	8.3
9:1	520	2800	188,662	5.4
8:2	513	2678	270,750	5.2
7:3	567	3375	368,351	6.0
5:5	476	3189	410,600	6.7
3:7	443	3155	396,725	7.1
0:10	300	894	17,230	2.98

Conditions: CHR feedstock (2.0 g, 40 mesh), solvent mixture (50.0 ml, EtOAc/H_2O = 10:0, 9:1, 8:2, 7:3, 5:5, 3:7, 0:10 (v/v)), 200 °C, 5 h

M_n, number average molecular weight; M_w, weight average molecular weight; M_z, Z-average molecular weight; D, dispersion degree, D = M_w/M_n

[a]refers to the result of GPC analysis, the value of M_n, M_w, M_z, D releated to the degree of depolymerization of lignin

fragments migration (Cai et al. 2013; Sluiter et al. 2008). Some research suggested that the medium polarity of the mixed solvents should contribute to the dissolution of lignin-based fragments. The polarities are similarity between the mixed solvents and lignin-based fragments (containing the nonpolar (aromatic rings, methoxy group and ether linkages) and polar groups (hydroxyl and aldehyde groups))(Shuai and Luterbacher 2016; Pouteau et al. 2005; Xue et al. 2016). While cellulose dissolution kept increasing with a strengthening characteristic vibrations of cellulose when the volume ratio increased from 10:0 to 0:10 (Fig. 1 and Fig. S1) and the M_w, M_n and D values of fragments decreased, except for 10:0 point (the lowest M_w, M_n and D values were responsible for a trace amount of dissolved cellulose) (Fig. S1 a). Therefore, it can be concluded that some portion of hydrogen bonds and ether linkages between lignin and cellulose were destroyed during this process. Meanwhile, in EtOAc/H_2O co-solvent system, EtOAc and H_2O could solvate lignin and cellulose fragments, respectively, inhibiting fragments repolymerization, and the interaction between fragments and solvents facilitated fragments further dissolution.

Effect of $MgCl_2$ and Ru/C on the cleavage of intermolecular linkages

To meet the high requirement of the cleavage of both intermolecular linkages between lignin and cellulose and intramolecular linkages in lignin, $MgCl_2$ and Ru/C were added for CHR degradation in biphasic EtOAc/H_2O (8:2). As shown in Table 2, $MgCl_2$ and Ru/C exhibited different effect on lignin and cellulose linkage cleavage in EtOAc/H_2O. In Ru/C case, 75.3% of lignin and 27.4% of cellulose conversion were gained (Table 2, entry 1), while only 27.5% of lignin but 84.1% of cellulose were converted over $MgCl_2$ (Table 2, entry 2). If both Ru/C and $MgCl_2$ were used, 76.4% of lignin was converted, accompanying with 97.2% of cellulose conversion. These indicate that much better efficiency for lignin dissolution over Ru/C and pretty much cellulose dissolution over $MgCl_2$. As both ESI and GPC results shown (Fig. S4 and Fig. 4), meanwhile, the molecular weight (M_w) of oligomer was under 600 g mol^{-1}, suggesting a large amount of intermolecular linkages in CHR were cleaved over Ru/C or/and $MgCl_2$.

The FT-IR absorption peaks assigned to lignin at 1705, 1602, 1514, 1479 and 1424 cm^{-1} (Long et al. 2015; Shu et al. 2015; Jiang et al. 2015) decreased dramatically when Ru/C catalyst was added (Fig. 2c, d). For cellulose, the intensity of the absorption peaks at 1377, 1159, 1112, 1057 and 896 cm^{-1} (Hu et al. 2014; Jiang et al. 2015) significantly decreased in the presence of $MgCl_2$ (Fig. 2b, d). These results imply that lignin and cellulose were released from CHR matrix and a little of them still stayed in DRS (Table 2 and Fig. 2). The peaks at 1326 and 1268 cm^{-1} are assigned to stretching vibration of G and S units, and 835 cm^{-1} is C–H out of plane deformation of G and S units. They almost disappeared and demonstrated that Ru/C promoted the dissolution of S and G units (Fig. 2c , d). However, a few S (ne), G (ne, e) resonance units were recorded, as well as $–OCH_3$ (derived from S (ne), G (ne, e) units) assigned at 55.0 ppm in the signal of ^{13}C CPMAS solid-state NMR (Table S7 and Fig. 3). This might be attributed to a little hydroxyl and acetyl groups in S and G units that lead to form the strong hydrogen bonds with cellulose and then stay in DSR in the form of S (ne), G (ne, e). However, Ru/C showed weak effect on cellulose dissolution with low cellulose conversion (Table 2 and Fig. 2). This is in line with previous results that only a little pentose and hexose from cellulose were obtained by converting the non-pretreated biomass with the use of Ru on carbon catalyst (Op de Beeck et al. 2013). Apparently, Ru/C was more favorable for lignin dissolution. As Fig. 3 and Table S7 shown, after $MgCl_2$ treating, the crystalline cellulose (C_6 ordered assigned at 65.0 ppm and C_4 ordered at 88.0 ppm) and amorphous cellulose (C_6 ordered assigned at 62.7 ppm and C_4 ordered at 84.0 ppm) nearly disappeared, proving that the crystalline and amorphous cellulose were converted in $MgCl_2$ case. This result is in agreement well with the XRD result of DSR (Fig.S3a, 3c and 3d). The fingerprint signal of ^{13}C CPMAS NMR at 105.0–160.0 ppm and 55.0 ppm demonstrate that a portion of lignin remained in DSR (Fig. 3 and Table S7). Thus, Ru/C and $MgCl_2$ are able to break the intermolecular linkages (ether bonds) between lignin and cellulose.

The characteristic absorbance peaks of lignin in DSR (Fig. 2B) were further decreased even disappeared, ascribing to more lignin (especially S (ne) and G (ne, e) fragments) and cellulose were removed by

Table 2 The effect of catalyst on CHR degradation (biphasic EtOAc/H_2O (8:2, v/v) solvents)

Entry	Catalyst	Conversion of feedstock[a] (wt%)	Residual solid[b] (wt%)	Lignin conversion (wt%)	Cellulose conversion (wt%)	Liquid weight yield (wt%)				Aqueous phase products[d] (g)
						EtOAc phase[c]				
						Linear alcohols/ esters	Volatile aromatics	Non-aromatic cyclics	Others (non-volatile)	
1	Ru/C	62.5	37.1	75.3	27.4	10.3	24.1	6.6	40.2	0.13
2	$MgCl_2$	40.5	58.8	27.5	84.1	18.7	7.9	16.9	18.9	0.53
3	Ru/C + $MgCl_2$	75.2	27.1	76.4	97.2	8.4	30.4	12.8	45.6	0.61
4	Ru/C + $MgCl_2$ (15 bar H_2)	80.6	18.5	81.5	98.5	9.2	37.5	14.5	28.8	0.67

Reaction Condition: 2.0 g of CHR (40 mesh), 0.5 g of 5 wt% Ru/C, 1.0 g of $MgCl_2 \cdot 6H_2O$, 50.0 mL of solvent mixture (EtOAc/H_2O = 4:1(v/v)), 200 °C, 5 h

[a]CHR conversion was determined via the weight comparison of initial and recovered residue (mass of Ru/C was subtracted)

[b]Based on the weight of feedstock

[c]The weight of volatile aromatics, linear alcohol/ester and non-aromatic cyclics were measured by internal standard method using acetophenone as standard compound; the weight of others (non-volatile) was weighed when the solvent was removed

[d]The weight of aqueous phase products was calculated after solvents were removed and the weight of $MgCl_2$ was subtracted

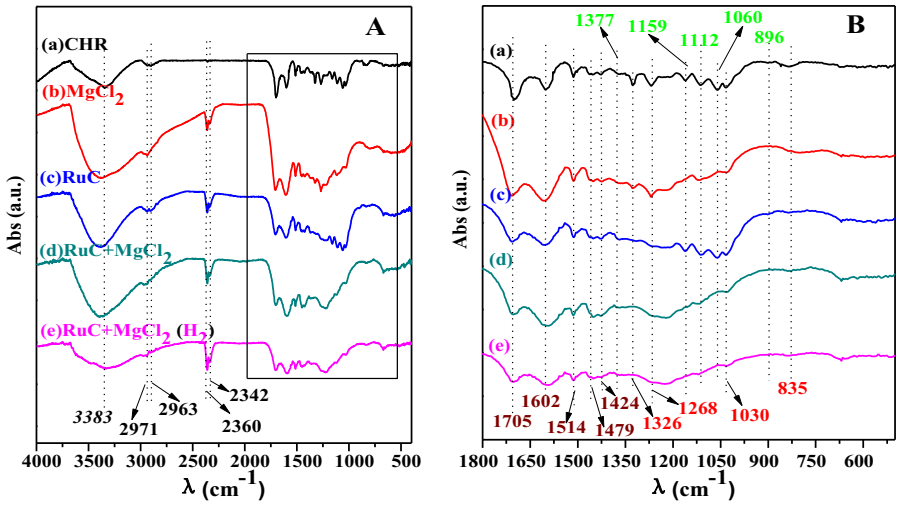

Fig. 2 FT-IR spectra of CHR and DRS (a) CHR; (b) $MgCl_2$; (c) Ru/C; (d) $MgCl_2$ + Ru/C; (e) $MgCl_2$ + Ru/C (H_2). Reaction condition: 2.0 g of CHR (40 mesh), 0.5 g of Ru/C (5 wt%), 1.0 g of $MgCl_2{\cdot}6H_2O$, 50.0 mL of solvent mixture (EtOAc/H_2O = 4:1(v/v)), 200 °C, 5 h

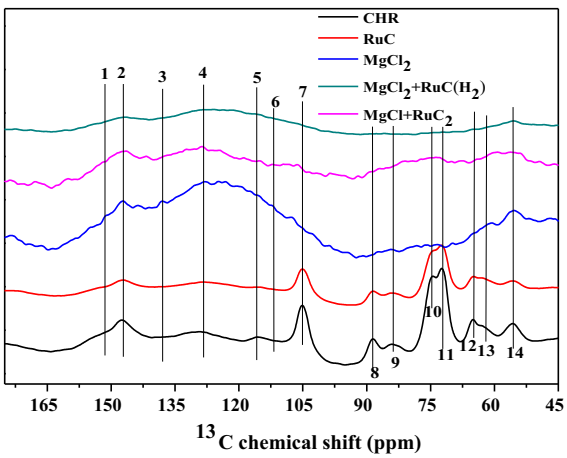

Fig. 3 ^{13}C CPMAS solid-state NMR spectra of CHR and DSR. Reaction condition: 2.0 g of CHR (40 mesh), 0.5 g of 5 wt% Ru/C, 1.0 g of $MgCl_2{\cdot}6H_2O$, 50.0 mL of solvent mixture (EtOAc/H_2O = 4:1(v/v)), 200 °C, 5 h

the synergetic effect of the Ru/C combined with $MgCl_2$ (Fig. 2d). These results were related to the weakening peak strength at 1030 cm^{-1} (C–O–C ether group) in Fig. 2a–d, corresponding to the breakage of intermolecular linkages of C–O–C ether group. However, a trace amount of S (ne) and G (ne, e) units were too recalcitrant to break in EtOAc/H_2O co-solvent over Ru/C combined with $MgCl_2$ (Table S7 and Fig. 3). In spite of reaction with external H_2, limited S (ne) and G (ne, e) were degraded. (Table 2 and Fig. 3). Therefore, intermolecular linkages (ether bonds) in CHR were nearly cracked by the synergetic effect of Ru/C combined with $MgCl_2$.

Effect of $MgCl_2$ and Ru/C on the cleavage of intramolecular linkages of lignin

Without Ru/C and $MgCl_2$, although lignin conversion reached the highest value (25.4%) in 8:2 case (Fig. 1), little monomer aromatic can be detected in organic phase (not give the GC–MS and GC results), suggesting that lignin fragments were dissolved as large molecular weight oligomers and limited lignin intramolecular linkage was cleaved.

The EtOAc phase liquid products, derived from Ru/C and $MgCl_2$ catalytic cleavage, were completely dissolved in THF solvent for GPC analysis (Fig. 4) and dissolved in methanol for ESI analysis (Fig.S7 and Table S10). The ESI analysis is used to detect the lignin fragment molecular weight (M_w). The result of GPC displayed that the molecular weight (M_w) of fragments below 600 g mol^{-1} and nearly no peak showed up more than m/z 600 in all cases (Fig. 4 and Fig. S4), implying that the linkage of lignin was broken to the narrow and small M_w distribution over $MgCl_2$ or/and Ru/C catalysts. Here, we combine the results of FT-IR (Figs. 2, 5), GC–MS (Table S1–4) and 2D HSQC NMR (Fig. S5b, Fig. S6b and Table S6) to conclude the probable structure of fragments for

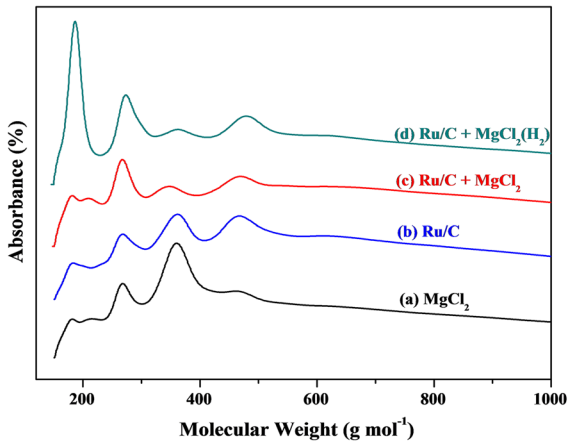

Fig. 4 GPC distribution of molar weight of non-volatile fraction in EtOAc phase over Ru/C and $MgCl_2$ catalyst reaction condition: 2.0 g of CHR (40 mesh), 0.5 g of 5 wt% Ru/C, 1.0 g of $MgCl_2{\cdot}6H_2O$, 50.0 mL of solvent mixture ($EtOAc/H_2O$ = 4:1(v/v)), 200 °C, 5 h

understanding the effect of $MgCl_2$ and Ru/C on the cleavage of linkages in lignin matrix.

For depolymerized lignin over $MgCl_2$, although 27.5% of lignin dissolved with the weaker absorbance peaks of lignin skeleton (Fig. 5a), the absorption peak assigned at C = C (2988 cm^{-1}) and 1654 cm^{-1}(-C = O) (carbonyl stretching in aryl aldehyde/acetone) are strong. They might be ascribed to the dehydration of HO-C_α-C_β to C_α = C_β bond, and followed retro-aldol cleavage of C_α = C_β to aromatic aldehydes in $MgCl_2$ case (Table S1, Fig. S5a and Fig. 6b) (Hu et al. 2014; Choi et al. 2016). The similar results of aldehyde signals were obtained from ^{1}H NMR analysis (δ_{H-} = 9.47 ppm, Fig. 6b). The main volatile aromatics are guaiacols and aromatic aldehydes (Table S1) in the volatile products of EtOAc phase. As for non-volatiles, a small number of fragments P_{CE}, P_{CE}, G and H were observed in $MgCl_2$ case (Fig. S7a). Similarly, a relative less m/z result was obtained (Fig. S4a). Form the result of ESI–MS analysis, the major β-O-4 and α-O-4 linkages in dissolved lignin fragments were broken over $MgCl_2$ (Fig. S4), leading to the formation of fragments (e.g., trimer fragments M_w= 532, 514, 510 g mol^{-1} and dimers fragments M_w = 458,392, 376, 360, 376, 348, 350, 242, 240, 218 g mol^{-1}) (Fig. 5, Fig.S5–S6, Table S10, Scheme 3). The formed trimer (e.g., M_w = 532, 514 g mol^{-1}) could be further converted to dimer (M_w = 348 g mol^{-1}) by the cleavage of β-O-4 and α–β linkages (Scheme 3(1–2)). Trimer fragment (M_w= 510 g mol^{-1}) might be fractured to dimer (M_w = 348/392 g mol^{-1}) by the cleavage of α-O-4 and γ-OH/α-O-4, β-O-4 and γ-5 linkages (Scheme 3(3–4)). Moreover, dimer fragments M_{w-} = 458, 348 and 376 g mol^{-1} could be accordingly fractured to monomers (M_w = 196, 166,152 g mol^{-1}) by the cleavage of α-O-4, β-O-4 and α-β linkages (Scheme 3(5–6)). For the strongest m/z (218), it can be

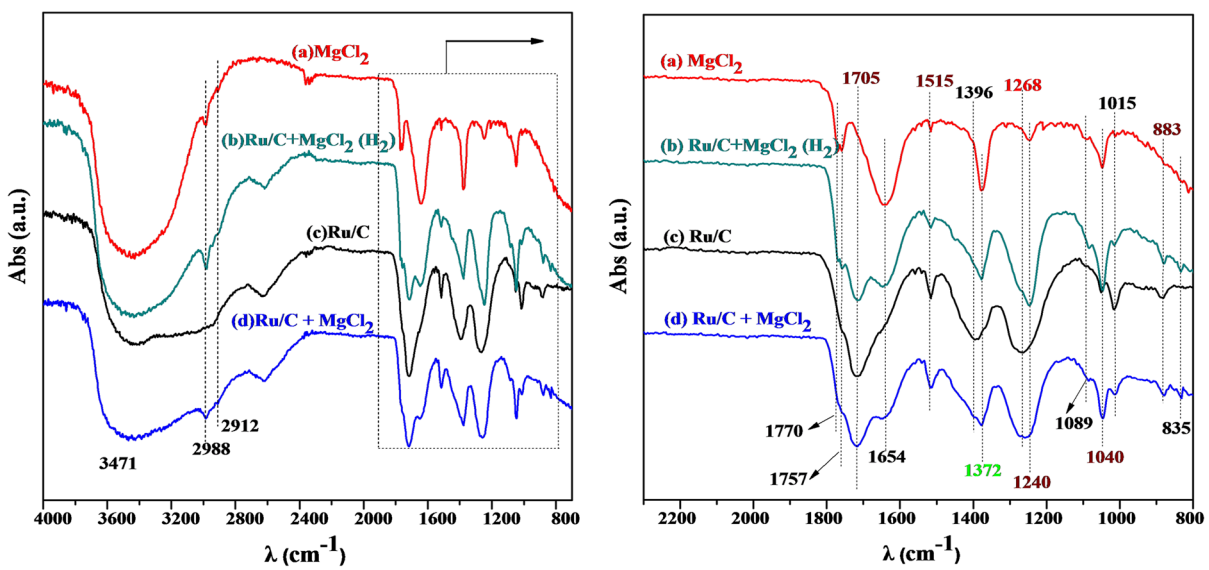

Fig. 5 Diffuse reflection FT-IR profile of fractions in organic phase over Ru/C and $MgCl_2$ catalyst. Reaction condition: 2.0 g of CHR (40 mesh), 0.5 g of 5 wt% Ru/C, 1.0 g of $MgCl_2{\cdot}6H_2O$, 50.0 mL of solvent mixture ($EtOAc/H_2O$ = 4:1(v/v)), 200 °C, 5 h

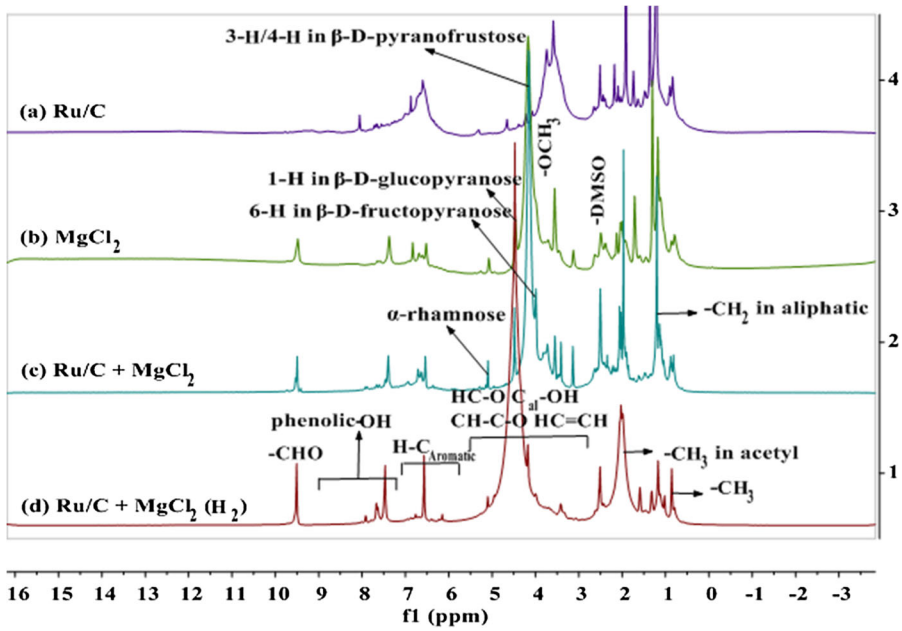

Fig. 6 ^{1}H NMR spectrum of non-volatile fractions from catalytic hydrogenolysis of CHR in EtOAc/H_2O co-solvents at 200 °C over (a) Ru/C, (b) $MgCl_2$, (c) Ru/C + $MgCl_2$, (d) Ru/C + $MgCl_2$ (H_2)

deduced as phenolic ester because the absorption peak at 1770 cm^{-1} assigned to phenol ester bond (Fig. 5a, Table S10). Therefore, it can be known that some α-O-4 and β-O-4 linkages and a small amount of bonds in the side chain (β-γ, α-β, γ-5 and γ-OH bonds) are cleaved in $MgCl_2$ case with 7.9% of volatile aromatics yield (Table 2). However, some α-O-4 and β-O-4 linkages still exist in the resultant oligomers (17.2%), indicating limited breakage of these linkages and chemical bonds under mild conditions over $MgCl_2$ catalyst.

About 24.1% of monomer aromatics and a set of oligomers (40.2%) were obtained in Ru/C case (Table 2), accompanying with the strong absorbance peaks of lignin (1705 and 1515 cm^{-1}) in Fig. 5c. It is shown that about 37.5% of the dissolved lignin existed as monomer aromatics with higher degree depolymerization. Correspondingly, the obvious C–O stretching vibration peaks of G (1268 cm^{-1}) and S (1326 cm^{-1}) units in FT-IR (Fig. 5) were observed and were in lined with the result of HSQC-NMR (Fig. S5b) and GC–MS analysis (Table S2). These demonstrate that Ru/C was more advantageous to the breakage of the intramolecular linkages in lignin, releasing a set of small M_w of H, G and S fractions. The monomer aromatics are mainly from G, H and some S units (Table S2), such as phenol, 2-methoxy-4-propyl-phenol, 2, 6-dimethoxy-4-propyl-phenol and some other aromatics. And the set of oligomers were P_{CE}, F_A, P_B, G, S', T, J_β, A, C, I and E fragments detected by 2D HSQC NMR analysis (Fig. S5b, Fig. S6b and Table S6).

Correspondingly, the result of ESI–MS analysis displayed that α-O-4, β-O-4 linkage might be cleaved to form fragments (e.g., trimers M_w= 514 and dimers M_w= 400, 392, 376, 360, 242 g·mol^{-1}). Meanwhile, the β-O-4, α-O-4, β-5 and 4-O-5 linkages as well as the bonds in the side chain of phenylpropane (e.g., α-β, α-OH,β-OH and γ-OH) could be greatly cleaved, indicating these linkages and side chain bonds were fractured under mild conditions. For instance, the β-O-4 linkages and α-β side chain bond in oligomer (M_w= 514 g·mol^{-1}) could be broken to form dimer (M_w= 392 g mol^{-1}) (Scheme 4(1)), and then the α-O-4 linkage and the side chain α-OH and β-OH bonds in dimer (M_w= 392 g mol^{-1}) might be fractured to obtain monomers (Scheme 4(3)). The α-O-4 and β-5 linkages of dimers (M_w= 400, 376, 284 and 242 g mol^{-1}) as well as α-OH or/and β-OH of side chain bonds, might be cleaved to obtain the monomers (Scheme 4 (2, 4, 6–8)). In addition, dimers with 4-O-5 linkage (e.g., M_w= 360 g mol-1) could be broken even under mild conditions (Scheme 4 (5)). The β-5 and 4-O-5 linkages were not found to break in $MgCl_2$ case. These above result demonstrate that the main portion of β-O-4, α-O-4, β-5 and 4-O-5 linkages and

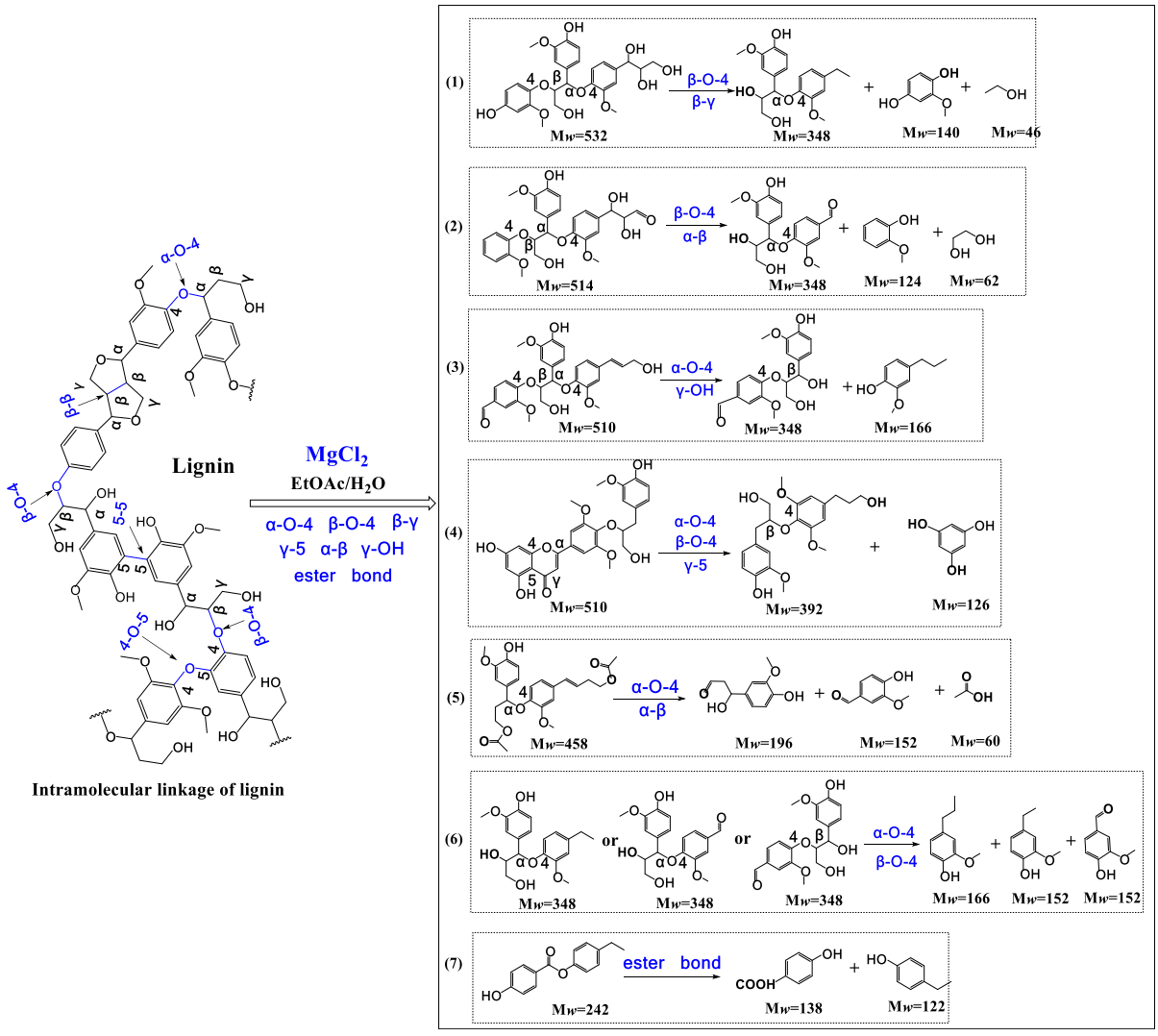

Scheme 3 The proposed pathway of the cleavage of intramolecular linkage in lignin over $MgCl_2$ catalyst in biphasic EtOAc/H_2O solvents

some part of α-β, α-OH and β-OH chemical bonds were cleaved by Ru/C in EtOAc/H_2O solvents under mild conditions.

When Ru/C combined with $MgCl_2$ for CHR catalytic degradation, tiny lignin signals was detected in the ^{13}C CPMAS NMR analysis of DSR (Fig. 3), and 76.4% of lignin was converted to 30.4% of volatile aromatics and 45.6% of lignin oligomers with the m/z of fragments below 500 (Table 2, Fig. 4 and Fig. S7c), suggesting the interaction between Ru/C and $MgCl_2$ could be readily cleaved more intramolecular linkages of lignin. The lignin matrix was broken to a large amount of P_{CE}, P_B, G, S, H, T, E, J, F_A, A and C fragments (Fig. 5c and Fig. S7c) and a large abundance of volatile monomer aromatics: phenols, guaiacols, syringaresinols and aromatic aldehydes/acetones, such as, guaiacol, 2-methoxy-4-vinylphenol, 2-metyoxy-4-propylphenol, 2,6-dimethoxy-4-propylphenol, trans-isoeugenol, 2,6-dimethoxy-4-(2-propenyl)-phenol, 3-(4-methoxyphenyl) propanal, and so on (Table S3). It's worth noting that a growing yield of G unit monophonic compounds and a higher yield of S unit monomers (2,6-dimethoxy-4-propylphenol, 2,6-dimethoxy-4-(2-propenyl)-phenol and 4-hydroxy-3,5-

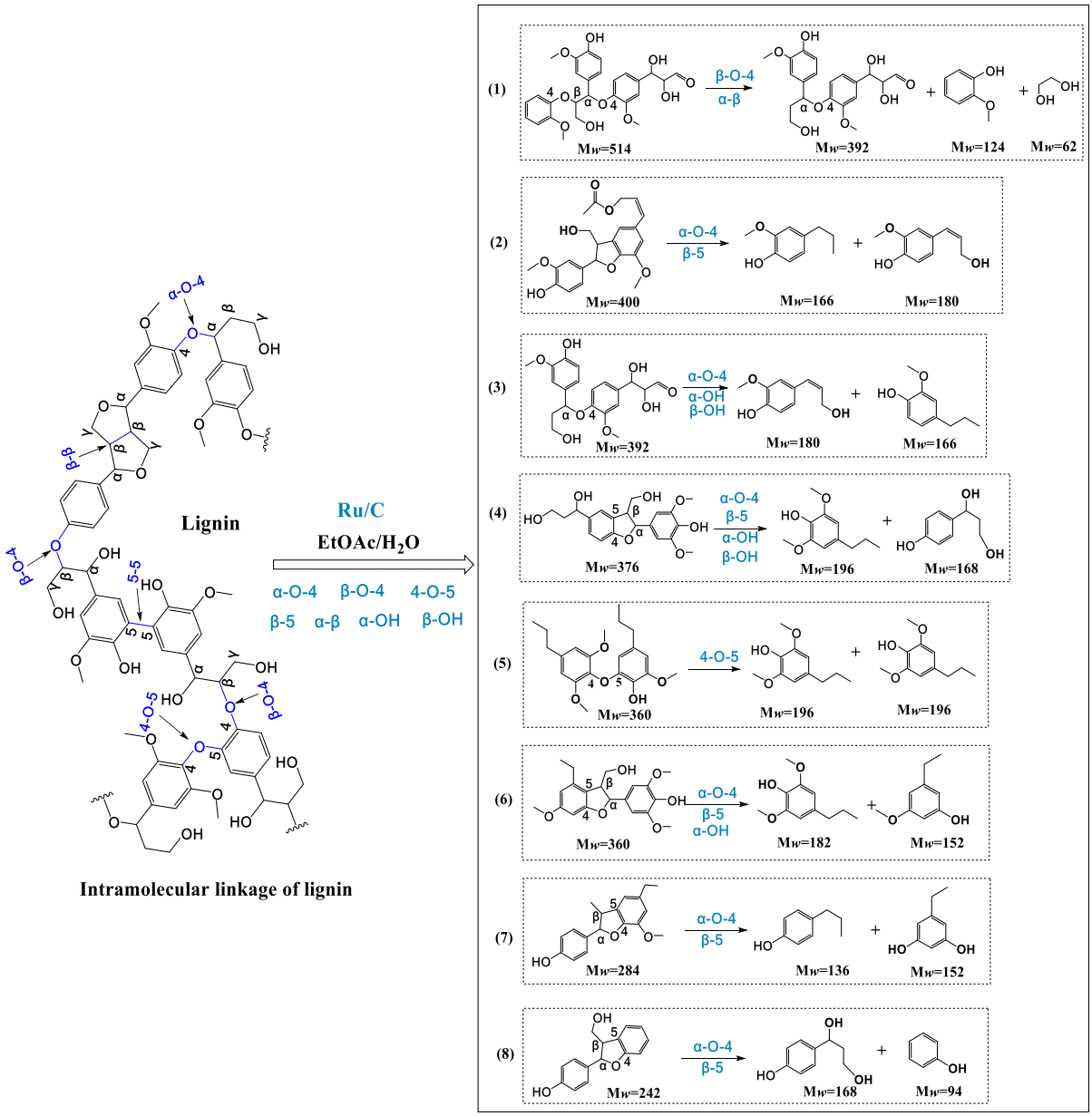

Scheme 4 The proposed pathway of the cleavage of intramolecular linkage in lignin over Ru/C catalyst in biphasic EtOAc/H_2O solvents

dimethoxy-benzaldehyde) in volatiles were given over Ru/C cooperated with $MgCl_2$ catalysts (Table S3). These are also well consistent with the results from FT-IR and HSQC-NMR spectrums. For instance, the strong C–O stretching vibration peaks of G and S units were detected in FT-IR spectra (Fig. 5d), and stronger fingerprint signals of G and S unit displayed in aromatic region (Fig. S5c). Thus, it was considered that a large number of oligomers and monomers of G and S units are related to synergetic effect of Ru/C and $MgCl_2$. Meanwhile, lots of aromatic aldehydes/acetones (C = O bonds) and unsaturated side chain of phenylpropane (C = C bonds) were obtained, which were not observed in Ru/C and $MgCl_2$ cases, implying that Ru/C combined with $MgCl_2$ showed the effect of promoting more fragments breakage by dehydration

and retrograde aldol reactions. Similar results were found by Marks.et al., where employing a weaker Lewis acid incorporated with the hydrogenation catalyst to remove reactive intermediates, resulting in higher yield of unsaturated products (Lohr et al. 2015). Besides, the C–O (ester bond in aromatic esters) stretching vibration at 1015 cm^{-1} are evident in both Ru/C and $MgCl_2$ cases (Fig. 5a, c), while it shows a weak stretching vibration when CHR degraded over Ru/C combined with $MgCl_2$. The result may be ascribed to the fact that esterification reaction was suppressed or some part of esters were hydrolysis in Ru/C incorporated with $MgCl_2$ case.

Compared to Ru/C case and $MgCl_2$ case, ESI–MS analysis showed that no trimer and a little dimer of ESI–MS signals (*e.g.,* m/z = 326, 312, 296 and 256) were detected in the organic phase products (Fig. S7c), suggesting the β-O-4, α-O-4, β-5 and 4-O-5 linkages in lignin were strongly broken over Ru/C cooperated with $MgCl_2$, as well as limited β-1 and 5-5 linkages. For example, the dimers (M_w= 326, 312 and 296 g mol^{-1}) might be also converted to monomer aromatics after the cleavage of α-O-4 and β-5 linkages (Scheme 5 (1–3)). The β-1 and 5-5 linkages in dimers (M_w = 256 g mol^{-1} and 216) could be further cleaved to form monophonic compounds (Scheme 5 (4 and 6)). Additionally, the signal at m/z 217 (H^+) were detected in the ESI–MS analysis of liquid products derived from $MgCl_2$ and Ru/C cases, which indicated that ester linkages in oligomers were not broken or generated, while this signal was not found in Ru/C incorporated with $MgCl_2$ case. This could be confirmed by the fact that ester linkage was cleaved (Scheme 5 (5)) or esterification reaction was inhibited over Ru/C combined with $MgCl_2$. Based on the aforementioned results, it can be known that Ru/C

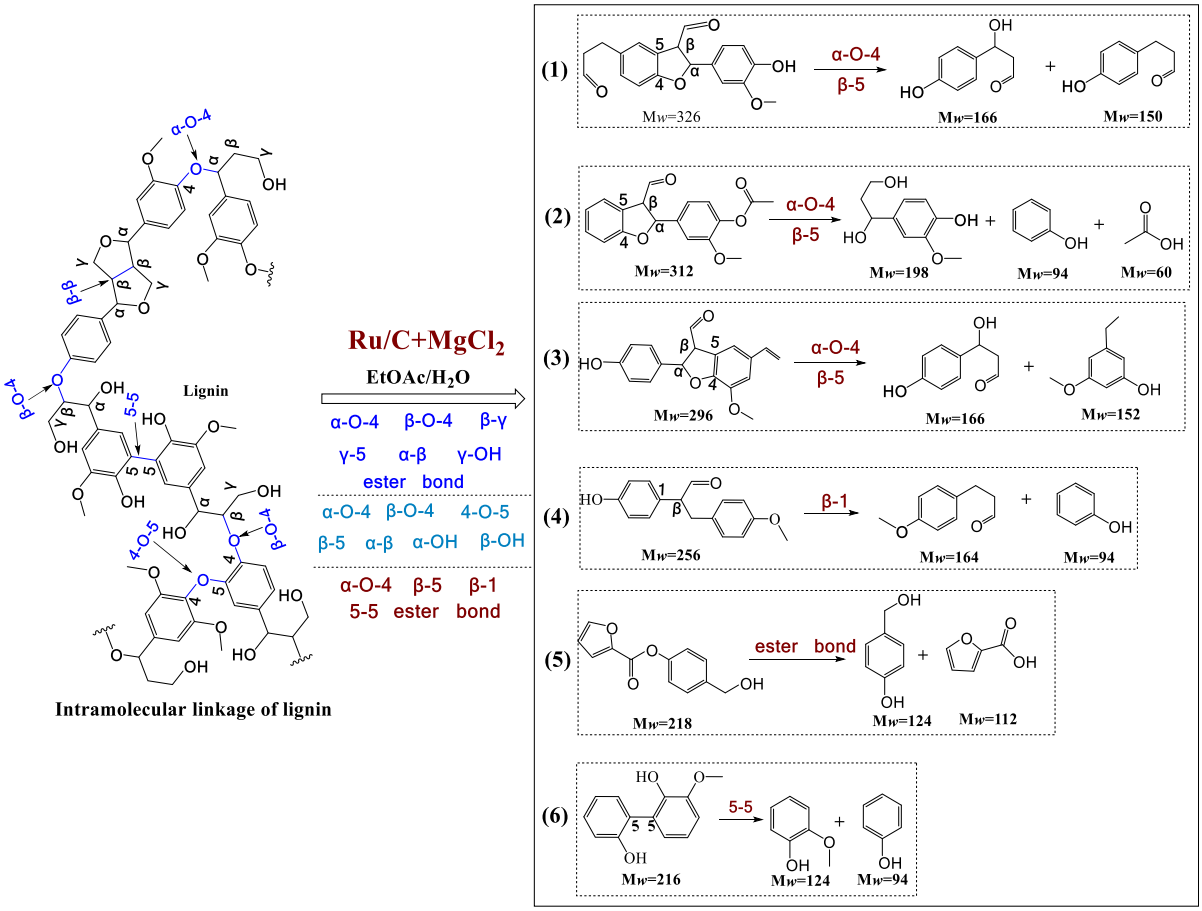

Scheme 5 The proposed pathway of the cleavage of intramolecular linkage in lignin over Ru/C + $MgCl_2$ catalyst in biphasic EtOAc/H_2O solvents

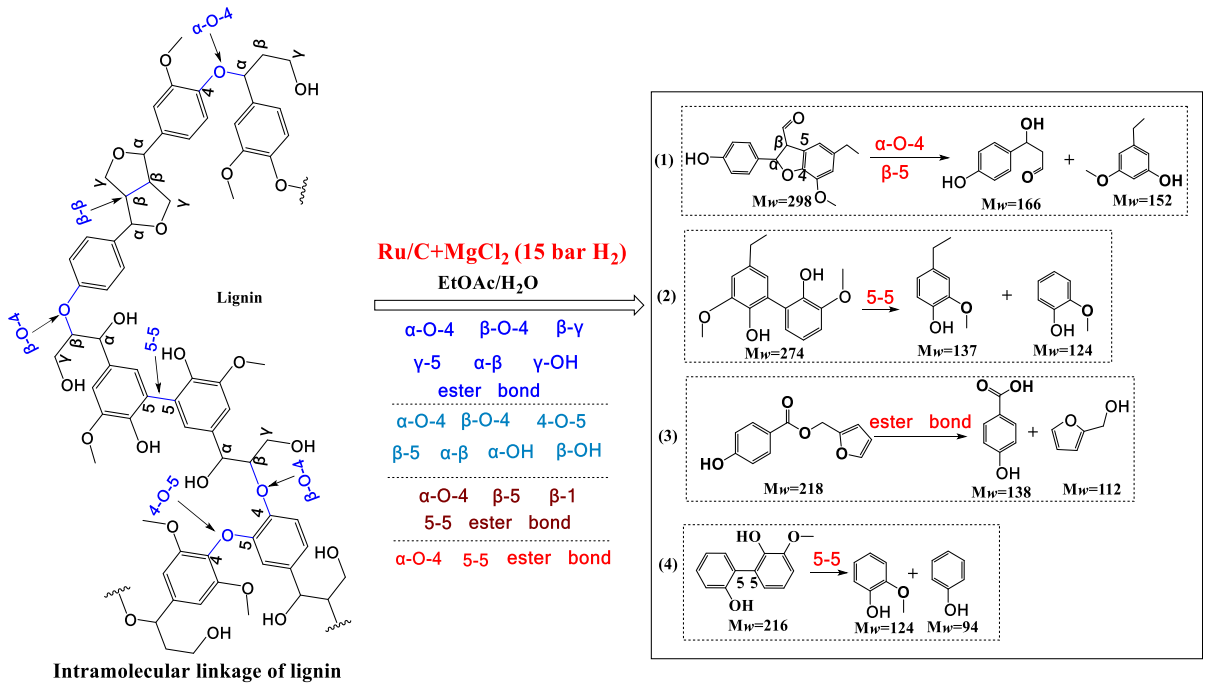

Scheme 6 The proposed pathway of the cleavage of intramolecular linkage in lignin over Ru/C + $MgCl_2$ catalyst in biphasic EtOAc/H_2O solvents under 15 bar H_2 pressure

combined with $MgCl_2$ shows the great efficiency for the cleavage of intermolecular linkages between lignin and cellulose, as well as the great efficiency in cleaving intramolecular linkages in lignin. Under mild conditions, pretty much all intramolecular β-O-4, α-O-4, β-5 and 4-O-5 linkages, some portion of α-β, β-γ, α-OH,β-OH and γ-OH bonds in the side chains, as well as limited β-1 and 5-5 linkages, can be cleaved to form oligomers and monomers. The synergistic effect of Ru/C combined with $MgCl_2$ showed effectively breakage of intramolecular linkages.

To know more about the stubborn linkages remained in DSR and to enhance lignin conversion, 15 bar H_2 pressure was added when CHR was deconstructed over $MgCl_2$ combined with Ru/C catalysts at 200 °C. About 10 bar pressure (H_2 occupied 98.8% of gas volume, Table S9) was retained after reaction. Although the lignin conversion slightly increased to 81.5% and the lignin fragments did not further cleave to smaller M_w (Entry 3 and 4 in Table 2), the lignin signal of S (ne, e)/G (ne, e) obviously decreased in DSR (Fig. 3 and Table S7). It was thereby inferred that the S (ne) and G (ne, e) oligomers were dissolved under tougher condition (H_2 pressure). Remarkably, the yield of monomer aromatics was increased, some C = C bonds in benzene ring and in the side chain of phenylpropane were hydrogenated, ascribing to more oligomers and C = C were converted by hydrogenation (Table 2 and Table S4). Correspondingly, H and E fragments disappeared and P_{CE}, F_A, P_B, S, G and T fragments clearly decreased (Fig. S5d), demonstrating the external H_2 further facilitated the cleavage of α-O-4, β-O-4, 4-O-5 and β-5 intramolecular linkages of lignin. Furthermore, the signal of S_1 (ne), S_4 (ne), S_5 (ne), G_4 (ne, e) and G_1 (ne) clearly decreased at 147.5 and 127.7 ppm in Fig. 3 ^{13}C CPMAS spectra (Fig. 3d, Table S7), which could be associated with the results of ESI–MS (Table S10): the fragments m/z = 298, 274, 218 and 216 g mol^{-1} were dissolved in organic phase and they might be further convert to monomer aromatics by breaking α-O-4 and β-5, 5-5 linkages and ester bonds (Scheme 6). On the other hand, the remained lignin in DSR is likely to S_1 (ne), S_3 (ne) and S_5 (ne) that might be from the oligomers with β-5, 5-5, β-1 and Ar–OH, indicating that some portion of stubborn β-5, 5-5, β-1 linkages are hard to cleaved even with the help of external H_2 pressure. Thus, the addition of external H_2 exhibited better efficiency for the breakage of β-5 and 5-5, intramolecular linkages in

lignin oligomers, as well as the hydrogenation of oligomers and C = C bond.

Effect of $MgCl_2$ and Ru/C on the cleavage of linkages in cellulose

Cellulose, a straight chain biopolymer, consists of glucose unit connected with β-1,4-glycosidic bonds, and aggregates to form three-dimensional crystal structure by intensive hydrogen bonds (Jiang et al. 2018). Expect for the linkage of β-1,4-glycosidic bond, the intramolecular hydrogen bonds (O(2)-H···O(6) and O(3)-H···O(5)) are also the linkages in the straight chain polymer of cellulose. While the intermolecular hydrogen bonds (O (6)-H···O (3′), O (6)-H···O (2′) and O (2)-H···O (2′)) as linkages connect the straight chain polymers (Scheme 2A) (Vispute et al. 2010; Jiang et al. 2016b, 2018; Oh et al. 2005; Kondo and Sawatari 1996; Dornath et al. 2015). Thus, the breaking of linkage is necessary for cellulose dissolution and conversion.

Without catalyst, cellulose was dissolved by EtOAc/H_2O co-solvent system (Fig. 1). With EtOAc/H_2O volume ratio decreasing, more cellulose intramolecular linkages cleaved with cellulose conversion increasing up to 21.4% at the point of 0:10 (Fig. 1, Table S6 and Fig. S1). The absorption peaks at 1374, 1057 and 896 cm^{-1} represent C–H bond of aliphatic, C–O bond and β-1,4-glycosidic bond in cellulose were dissolved (Fig. S1). It could be seen that the combined action of ethanol, acetic acid (from EtOAc hydrolysis) and H_2O could break the ester bonds of LCC (Scheme 2). These may be ascribed to H_3O^+ (especially more H_2O was used) and the anions (OAc^-, $HCOO^-$) that play important role in the breaking of inter- and intramolecular linkages to facilitate cellulose dissolution (Vitz et al. 2009; Wang et al. 2012). Thus, EtOAc/H_2O solvents were favorable for the cleavage of the intermolecular linkages between cellulose and lignin, and then promoted the simultaneous conversion of these two components.

When Ru/C or/and $MgCl_2$ were added to CHR depolymerization, lots of fragments from cellulose were released in aqueous phase. The molecular weight distribution of aqueous soluble product was m/z = 59–1034 and the common compounds were $C_6H_6O_4$, $C_6H_{14}O_7$, $C_8H_{16}O_7$, $C_{16}H_{32}O_2$ and $C_{18}H_{36}O_2$ in all cases (Fig. S7), suggesting that the aqueous soluble fractions are mainly cellulose degradation products, a small amount of lignin fragment, long chain aliphatic ester and acid. Meanwhile, some fragments derived cellulose were collected in organic phase (Fig. 5, Fig. S5–S6). The detail signal of fragments are given by ^{1}H-NMR spectra (Fig. 6) and ^{1}H-^{13}C HSQC NMR spectra of non-volatile fractions (Fig. S6, Fig. 6, Table S6). The fragment units of β-D-glucopyranose, β-D-pyranofrustose and α-rhamnose were detected in non-volatiles. Except for oligomers, the monomeric products from cellulose were also detected in organic phase by GC–MS and the aqueous phase products by HPLC analysis (Table 2, Table 3 and Table S1–4). In all of cases, the predominant liquid products (both of aqueous and organic phases) were cellobiose, glucose, anhydro-sorbitol/mannitol, hydroxymethyl-furfural (HMF), 2-methyl-5-Furan-carboxaldehyde (2-Me–THF) (Table S2 and Table 3). As for linear products, levulinic acid (LA), levulinic acid ester (LAE), 1, 3-propylene glycol, ethylene glycol (EG) and long-chain aliphatic acid esters are the main fractions in EtOAc phase,and sorbitol, 1,3-propylene glycol, ethylene glycol (EG) and glycerinum in aqueous phase. According to the literature, it was supposed that furfural and HMF were derived from cellulose through dehydration, sorbitol and mannitol were produced by hydrogenation of C6 sugars. LA was obtained from HMF by hydration; 1, 3-propylene glycol, ethylene glycol and glycerinum were from the C–C bond splitting of sorbitol/mannitol over Ru/C; and it was supposed that lactic acids might be produced from cellulose (Geboers et al. 2011a; Liang et al. 2011; Liao et al. 2014). Additionally, it should be mentioned that some cycles (1,3:2,4-Dimethylene-d-epirhamnitol, 2,4:3,5-Dimethylene-l-iditol and tetrahydro-[1,3] dioxino [5,4-α] [1,3]dioxin-4-yl) ethylacetate) were found and extracted when Ru/C was used (Table 2, Table S2–5). Which derived from the aldol reaction occurred between sugar polyols and formaldehyde (formed during lignin depolymerization process) (Onwudili and Williams 2014; Pandey and Kim 2011; Sluiter et al. 2008).

From the FT-IR analysis of the fractions in aqueous phase, no β-1,4-glycosidic bond was detected in all cases (Table S5 and Fig. 7). It is thereby inferred that the fragments didn't contained β-1,4-glycosidic linkages broken by Ru/C or/and $MgCl_2$. While the intramolecular hydrogen bonds for O(2)-H···O(6) and O(3)-H···O(5), and the intermolecular hydrogen bonds for O(6)-H···O(3′) in cellulose appeared at 3455–3410,

Table 3 HPLC analysis of the component of fraction in aqueous phase

Compound	Retention time (min)	Mass (mg)			
		Ru/C	$MgCl_2$	Ru/C + $MgCl_2$	Ru/C + $MgCl_2$ (15 bar H_2)
Total non-volatiles[a]	–	130	532	611	670
Cellobiose	13.4	19.3	38.7	35.7	18.4
Glucose	15.6	32.8	97.6	105.5	99.4
Arabinose	16.1	1.0	1.5	2.4	1.5
Xylitol	16.2	–	2.9	1.6	1.9
Sorbitol	16.8	12.5	43.8	63.6	70.8
Erythritol	18.6	3.0	14.8	24.0	32.3
Lactic acid	19.8	3.1	22.3	26.3	40.5
Glycerinum	20.6	11.6	5.8	25.5	51.7
EG	23.8	12.7	4.2	25.4	37.6
Levulinic acid	24.2	3.4	41.3	48.6	56.8
HMF	44.3	4.5	72.2	81.5	116.4
Others[b]	–	26.1	186.9	160.9	142.9

General condition: 2.0 g of CHR (40 mesh), 0.5 g of 5 wt% Ru/C, 1.0 g of $MgCl_2{\cdot}6H_2O$, 50.0 mL of solvent mixture (EtOAc/H_2O = 4:1(v/v)), 200 °C, 5 h

[a]The mass of non-volatiles in aqueous phase was obtained after removing solvents and low molecular weight fractions

[b]Others contained unknown compounds in HPLC spectrum and the fractions could not detect by SH-1011 column

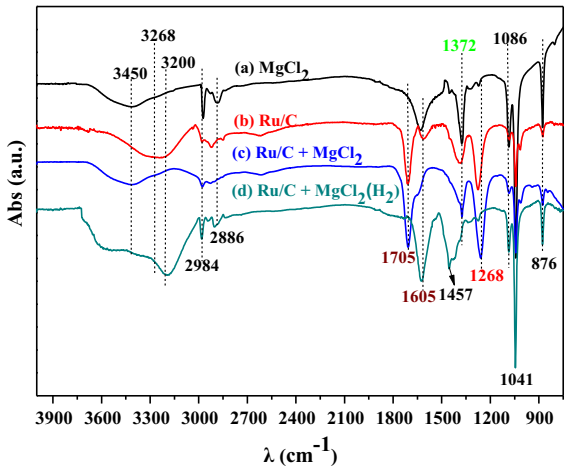

Fig. 7 Diffuse reflection FT-IR profile of fractions in aqueous phase over Ru/C and $MgCl_2$ catalyst. Reaction condition: 2.0 g of CHR (40 mesh), 0.5 g of 5 wt% Ru/C, 1.0 g of $MgCl_2{\cdot}6H_2O$, 50.0 mL of solvent mixture (EtOAc/H_2O = 4:1(v/v)), 200 °C, 5 h

3375–3340, and 3310–3230 cm^{-1}, respectively (Oh et al. 2005; Kondo and Sawatari 1996; Schwanninger et al. 2004),implying that the intra- and intermolecular hydrogen bonds of O(2)-H···O(6), O(3)-H···O(5) and O(6)-H···O(3′) were not completely cleaved and were collected in aqueous phase.

In Ru/C case, 27.4% of cellulose was converted to 0.13 g of aqueous products (Table 3), and the rest of cellulose in DSR is cellulose I with distinct XRD diffraction peaks (Fig. S3, the characteristic peaks at 2θ = 14.8°, 16.5°, 22.8° and 34.6° were ascribed to the (101), (10i), (002) and (040) lattice planes of cellulose, respectively) (Liao et al. 2014; Liu et al. 2015). This can well explain why a little of cellulose degraded product was collected in aqueous phase and organic phase. (Fig. S6b, Fig. 6a, Tables 2 and 3). However, a decreased signal of cellulose in DSR (the signals of C_1–C_5 range from 60 to 110 ppm, Fig. 3a, b) demonstrates that Ru/C made an effect on breaking the β-1, 4-glycosidic linkage and some portion of inter- or/and intramolecular hydrogen bond of cellulose. Meanwhile, the linkages (O(2)-H···O(6) (intra-), O(3)-H···O(5) (intra-) and O(6)-H···O(3′) (inter-)) suggested these intra- and intermolecular hydrogen bonds were not completely cleaved (Fig. 7 and Table S5) (Oh et al. 2005; Kondo and Sawatari 1996; Schwanninger et al. 2004). Therefore, β-1, 4-glycosidic linkage and some portion of inter- or/and intramolecular hydrogen bonds were fractured over Ru/C in in biphasic EtOAc/H_2O

solvents, releasing polysaccharose, cellobiose, glucose, anhydrosugar and sorbitol fragments, and so forth (Table 3 and Table S1). Meanwhile, a part of fragments were further cleaved to pentanoic acid, EG, 1,3-propylene glycol and glycerinum by breaking C–C linkages in cellulose. The rupture of cellulose linkage were dependent the reactions of hydrolysis and dehydration, and then converted to the corresponding polyols by hydrogenation, accompanying hydrogenolysis to short linear fractions by the C–C bond cleavage of sorbitol/mannitol over Ru/C in biphasic solvent (Scheme 7).

High cellulose conversion (84.1%) was given when CHR was treated with $MgCl_2$, resulting in the diffraction peak of cellulose nearly disappeared (Fig. S3c) and weak signal remained in ^{13}C CPMAS solid-state NMR (Table S7 and Fig. 3). These were attributed to a lot of the inter- and intramolecular hydrogens and β-1,4-glycosidic bonds of cellulose was cleaved over $MgCl_2$, as well as the sugar ring (Scheme 2A). In the presence of $MgCl_2$, the strong absorption peak at 3455–3200 cm^{-1} were attributed to the linkages of hydrogen bond (O(2)-H···O(6) (intra-), O(3)-H···O(5) (intra-) and O(6)-H···O(3′) (inter-)) in fragments, implying they didn't completely cleaved as in $MgCl_2$ case (Fig. 7 and Table S5) (Oh et al. 2005; Kondo and Sawatari 1996; Schwanninger et al. 2004). The cleavage of these linkages resulted in obtaining a large number of polysaccharose, β-D-pyranofrustose, cellobiose, glucose, sorbitol, erythritol, HMF, LA, and others (Table 3, Table S1). This can well explain why the highest yield of cycle products (16.9%) and linear fractions (18.7%) were given in organic phase (Table 2). The cycles are mainly cellobiose, glucose, mannitol, HMF, furfural, and 1, 6-anhydro-β-D-glucopyranose, and liner products are a larger amount of

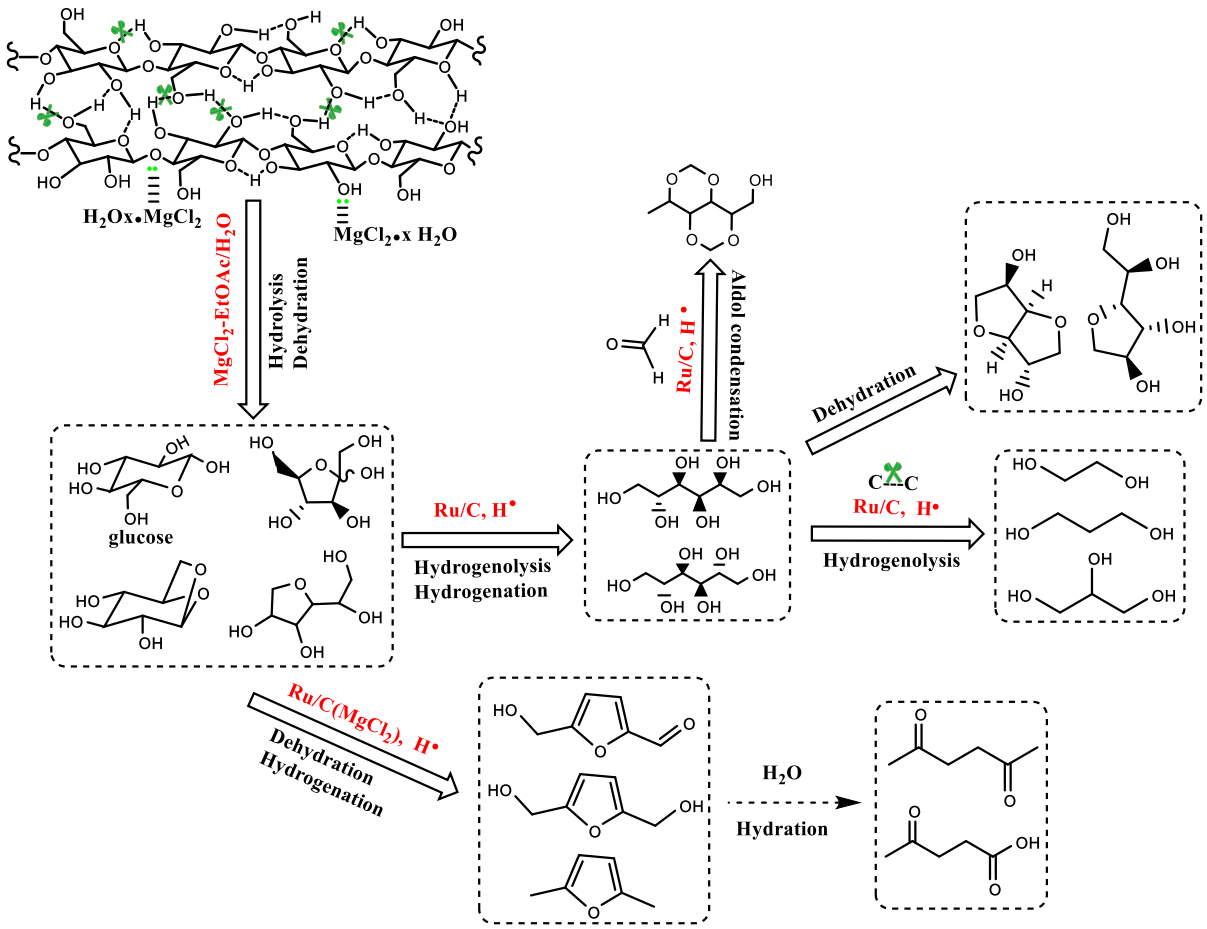

Scheme 7 Proposed cleavage linkage and reaction of cellulose matrix with Ru/C + $MgCl_2$ in biphasic EtOAc/H_2O solvent

LAE (LA) and long-chain aliphatic acid esters in both liquid phases (Table 3 and Table S1). The beneficial role of $MgCl_2$ in break down cellulose structure was exhibited in this work(Amarasekara and Ebede 2009). $MgCl_2$ provided Lewis acid site for the dehydration of carbohydrates because the isomerization of aldose (xylose or glucose) to ketose (xylulose and fructose) was the first step for the dehydration of the carbohydrates (Liu et al. 2015). Apparently, more glucose and sorbitol were afforded to convert to HMF and LAE (LA) in $MgCl_2$ case. These are plausible to suggest that the rupture of intramolecular linkages (hydrogen and glucosidic bonds) in cellulose are strongly dependent $MgCl_2$.

The strong cleavage ability of $MgCl_2$ could be ascribed to Mg^{2+} coordinated to all types of oxygen atoms (hydroxyl oxygen, ring oxygen and β-1, 4-glycosidic oxygen) of cellulose in aqueous solution (Rondeau et al. 2003; Yu et al. 2014; Sen et al. 2013). That is, the coordination of Mg^{2+} to the vicinal hydroxyl oxygen may weaken the hydrogen-bonding networks in cellulose, giving rise to the increased the formation of sugar oligomers at low temperature. The coordination of Mg^{2+} to glycosidic oxygen may catalyze the cleavage of β-1, 4-glycosidic bond to increase the formation of anhydro-sugar oligomers. For Mg^{2+} coordinates to ring oxygen, it may catalyze the ring-opening reactions, resulting from the destruction of sugar ring structures and promoting the formation of low-molecular weight products (Sen et al. 2013). These types of oxygen–Mg^{2+} coordination could lower the activation energy of the reaction (Amarasekara and Ebede 2009). Meanwhile, glucose also undergone rearrangement and dehydration to form the isolated furan derivatives. Thus, $MgCl_2$ made a great effect on breaking β-1, 4-glycosidic bond, lots of inter- and intramolecular hydrogen bonds, sugar ring and C–C linkages in the degraded fragment of cellulose.

As shown in Figs. 2d and 3, when Ru/C combined with $MgCl_2$, the FT-IR absorption peaks and NMR fingerprint signal of cellulose nearly disappeared in DSR. This is agreement well with the high cellulose conversion (97.2%) with 0.61 g of aqueous products (removed solvents, Table 3). At the same time, the oligomers of β-D-pyranofrustose, α-rhamnose and cellobiose, and the monomers of sorbitol, glucose, LA, HMF, erythritol, lactic acid, EG, glycerinum and 2,5-dimethylfuran were detected in aqueous phase and organic phase (Fig. 6, Table 3 and Table S3). Compared to the case of $MgCl_2$ or Ru/C, the yield of sorbitol, glucose, erythritol, LA, HMF and lactic acid increased, especially, EG and glycerinum obviously increased (Table 3, Table S1 and S3). For β-D-pyranofrustose, α-rhamnose and β-D-glucopyranose, stronger fingerprint signal was observed than that of $MgCl_2$ and Ru/C cases, particularly, the appeared signal of β-D-glucopyranose (Fig. 6b, c). While the yield of others decreased (Table 3). These above results demonstrate that the linkage of β-1,4-glycosidic, inter- and intramolecular hydrogen bonds and C–C in C5/C6 sugars were significantly broken. The evidently increased yield of product and the decreased content of oligomers (others, Table 3) were attributed to the synergistic effect of Ru/C combined with $MgCl_2$ on cleaving linkages. For instance, as shown in Fig. 7c, the weak O–H stretching vibration at 3320–3000 cm^{-1} demonstrated the synergistic effect nearly destroyed the intermolecular hydrogen bonds (O(6)H–O(3′), O(2)H–O(2′)(inter) and O(6)H–O(2′)), as well as the hydrogen bond linked to β-D-glucopyranose (Fig. 6c). The synergistic effect gave rise to break the C–C linkages of C5/C6 sugars/polyhydric alcohols to release EG, glycerinum, and so forth. Moreover, the synergistic effect also contributes to the dehydration of β-D-pyranofrustose (β-D-glucopyranose) to HMF and the hydration of HMF to LA.

When external H_2 pressure was added in the reaction system, 98.5% of cellulose was converted, which was in line with the very weak FT-IR absorption peak and NMR fingerprint signal of cellulose in DSR (Table 2, Figs. 2e, 3). Compared to Ru/C combined with $MgCl_2$ case, in the presence of H_2 pressure, the significant β-D-glucopyranose signal appeared and β-D-pyranofrustose nearly disappeared in organic phase (Fig. 6d), ascribing to the isomerization of β-D-pyranofrustose (Resch et al. 2013). The large broad peak (3000–3750 cm^{-1}) suggested that more OH-groups generated from glycosidic linkage and hydrogen bond hydrogenolysis. Furthermore, higher content of main products of β-D-glucopyranose, sorbitol, erythritol, LA, HMF, lactic acid, EG and glycerinum were given than that in Ru/C combined with $MgCl_2$ case. While the yield of cellobioser, glucose and others were decreased due to hydrogenation and hydrogenolysis (Table 3). These could be concluded that H_2 pressure is further contributed to cleave linkage of β-1,4-glycosidic bond, inter- and intramolecular

hydrogen bonds, sugar ring and C–C linkages of cellulose. At the same time, the unsaturated C = C bonds of the products were hydrogenated under H_2 pressure (Table S4).

The proposed cleavage of cellulose linkage and reaction for Ru/C combined with $MgCl_2$ are shown in Scheme 7. $MgCl_2$ plays a key role in the degradation of cellulose at 200 °C. Frist, a loose complex formed when cellulose was reacted with $MgCl_2$ aqueous solution. That is, a coordination bond formed between Mg^{2+} and the oxygen atom in β-1,4-glycosidic, and the hydrogen bonds of cellulose were detached by Cl^-. The coordinated water molecules from $MgCl_2{\cdot}6H_2O$, as a nucleophile, participated in the breakage of β-1,4-glycosidic bond to release glucose and oligomer (Scheme 4). On the other hand, another coordination bond also formed between Mg^{2+} and the vicinal hydroxyl group of glucose, which made glucose form an enediol intermediate structure to fructose by isomerization(Xu and Chen 1999; Richards and Williams 1970). At the same time, glucose also went through rearrangement, dehydration and hydration to furfural, HMF, LA, and so forth. Mg^{2+} also coordinated to ring oxygen and catalyzed the ring-opening reaction, resulting in the destruction of sugar ring structures and facilitating the formation of low-molecular weight products (Sen et al. 2013). These types of oxygen–Mg^{2+} coordination could lower the activation energy of the reactions. Although Ru/C showed a certain effect on breaking β-1,4-glycosidic bond and hydrogen bond, the cleavage of linkages in cellulose were mainly dependent $MgCl_2$ when they were used together. In the presence of Ru/C, hydrogenolysis and hydrogenation of C5/C6 sugar were conducted to EG, 1, 3-propylene glycol and glycerinum due to the splitting of C–C bonds. Much more β-1,4-glycosidic linkages, inter- and intramolecular hydrogen bonds, sugar ring and C–C bond were cleaved when Ru/C combined with $MgCl_2$ for cellulose degradation, much more glucose, sorbitol erylhritol, lactic acid, LA, HMF, glycerinum and EG were obtained.

Conclusions

Ru/C cooperated with $MgCl_2$ exhibited efficient effect on the cleavage of intermolecular linkages of LCC and intramolecular linkages of lignin and cellulose in CHR in biphasic EtOAc/H_2O solvents. After the destruction of linkages, a large amount of inter-/intramolecular linkages were destroyed under 200 °C, 80.6% of lignin and 98.5% of cellulose were separated and converted with 37.5 wt% of monomer aromatics and 28.8% of oligomers, as well as a large amount of non-volatile aqueous products. Concerning the intermolecular linkages, the effect of biphasic EtOAc/H_2O solvents mainly displayed on the cleavage of intermolecular linkages (hydrogen and ether bonds) in CHR. $MgCl_2$ showed limited abilities of breaking the α-O-4 and β-O-4 linkages in lignin and limited β-1, 4-glycosidic and hydrogen bonds in cellulose were cleaved over Ru/C catalyst. In terms of intramolecular linkages in lignin, $MgCl_2$ showed the effect on destroying C-O linkages (α-O-4,β-O-4 and ester bond) and C–C bonds of the side chain of benzene ring (α-β,β-γ and γ-5). Where the linkage of α-O-4 or/and β-O-4 were cleaved by ester bond hydrolyzed, the hydroxyl group in the aliphatic side-chain of lignin was prone to dehydrating to $C_\alpha = C_\beta$ bond and to cleaved $C_\alpha = C_\beta$ bond to aromatic acetones/aldehydes by retro-aldol reaction. The cleavage of the major linkages of β-O-4, α-O-4, β-5 and 4-O-5 linkages and some portion of α-β, α-OH, β-OH and γ-OH linkages were controlled by Ru/C catalyst, releasing a lot of G and H units and a part of S unit fragments. The synergetic effect between Ru/C and MgCl2 significantly facilitated the cleavage of intramolecular C–O and C–C linkages (α-O-4,β-O-4, 4-O-5, α/β-OH and α-β, β-5, β-1, 5-5) with a lot of H, G and S units. In the presence of H_2 pressure, more H, G and S units were given. In regard to the linkages of cellulose, $MgCl_2$ preferentially broken β-1, 4-glycosidic linkage, inter- and intramolecular hydrogen bonds and sugar rings. While Ru/C with H· exhibited the effect on C5/C6 sugar polyols hydrogenolysis and hydrogenation, as well as the rupture of C–C of polyols. The linkage of β-1, 4-glycosidic, inter- and intramolecular hydrogen bonds and C–C in C5/C6 sugars were significantly broken to evidently increased yield of products due to the synergistic effect between Ru/C and $MgCl_2$. Moreover, much C–C bond in C5/C6 sugars was disrupted in the presence of H_2 pressure. This work might provide useful information for hydrolysis residue depolymerization.

Acknowledgments This work was supported by NSFC (Natural Science Foundation of China) project (No. 51606205,

51676191, 51536009). Basic scientific research operating expenses project of Key Laboratory of Biomass Energy and Material, Jiangsu Province (JSBEM201902).

References

Amarasekara AS, Ebede CC (2009) Zinc chloride mediated degradation of cellulose at 200 degrees C and identification of the products. Bioresour Technol 100(21):5301–5304. https://doi.org/10.1016/j.biortech.2008.12.066

Bolker HI (1963) A lignin carbohydrate bond as revealed by infra-red spectroscopy. Nature 197(486):489–490. https://doi.org/10.1038/197489a0

Cai CM, Zhang TY, Kumar R, Wyman CE (2013) THF co-solvent enhances hydrocarbon fuel precursor yields from lignocellulosic biomass. Green Chem 15(11):3140–3145. https://doi.org/10.1039/c3gc41214h

Chheda JN, Huber GW, Dumesic JA (2007) Liquid-phase catalytic processing of biomass-derived oxygenated hydrocarbons to fuels and chemicals. Angew Chem Int Ed 46(38):7164–7183. https://doi.org/10.1002/anie.200604274

Choi YS, Singh R, Zhang J, Balasubramanian G, Sturgeon MR, Katahira R, Chupka G, Beckham GT, Shanks BH (2016) Pyrolysis reaction networks for lignin model compounds: unraveling thermal deconstruction of beta-O-4 and alpha-O-4 compounds. Green Chem 18(6):1762–1773. https://doi.org/10.1039/c5gc02268a

De Bruyn M, Fan J, Budarin VL, Macquarrie DJ, Gomez LD, Simister R, Farmer TJ, Raverty WD, McQueen-Mason SJ, Clark JH (2016) A new perspective in bio-refining: levoglucosenone and cleaner lignin from waste biorefinery hydrolysis lignin by selective conversion of residual saccharides. Energy Environ Sci 9(8):2571–2574. https://doi.org/10.1039/c6ee01352j

de Clippel F, Dusselier M, Van Rompaey R, Vanelderen P, Dijkmans J, Makshina E, Giebeler L, Oswald S, Baron GV, Denayer JF, Pescarmona PP, Jacobs PA, Sels BF (2012) Fast and selective sugar conversion to alkyl lactate and lactic acid with bifunctional carbon-silica catalysts. J Am Chem Soc 134(24):10089–100101. https://doi.org/10.1021/ja301678w

Deuss PJ, Scott M, Tran F, Westwood NJ, de Vries JG, Barta K (2015) Aromatic monomers by in situ conversion of reactive intermediates in the acid-catalyzed depolymerization of lignin. J Am Chem Soc 137(23):7456–7467. https://doi.org/10.1021/jacs.5b03693

Dornath P, Cho HJ, Paulsen A, Dauenhauer P, Fan W (2015) Efficient mechano-catalytic depolymerization of crystalline cellulose by formation of branched glucan chains. Green Chem 17(2):769–775. https://doi.org/10.1039/c4gc02187h

Ferrini P, Rinaldi R (2014) Catalytic biorefining of plant biomass to non-pyrolytic lignin bio-oil and carbohydrates through hydrogen transfer reactions. Angew Chem Int Ed 53(33):8634–8639. https://doi.org/10.1002/anie.201403747

Galkin MV, Samec JS (2014) Selective route to 2-propenyl aryls directly from wood by a tandem organosolv and palladium-catalysed transfer hydrogenolysis. Chemsuschem 7(8):2154–2158. https://doi.org/10.1002/cssc.201402017

Galkin MV, Samec JSM (2016) Lignin valorization through catalytic lignocellulose fractionation: a fundamental platform for the future biorefinery. Chemsuschem 9(13):1544–1558. https://doi.org/10.1002/cssc.201600237

Galkin MV, Dahlstrand C, Samec JSM (2015) Mild and robust redox-neutral Pd/C-catalyzed lignol -O-4 bond cleavage through a low-energy-barrier pathway. Chemsuschem 8(13):2187–2192. https://doi.org/10.1002/cssc.201500117

Gandini A (2011) The irruption of polymers from renewable resources on the scene of macromolecular science and technology. Green Chem 13(5):1061–1083. https://doi.org/10.1039/c0gc00789g

Geboers J, Van de Vyver S, Carpentier K, Jacobs P, Sels B (2011a) Hydrolytic hydrogenation of cellulose with hydrotreated caesium salts of heteropoly acids and Ru/C. Green Chem 13(8):2167–2174. https://doi.org/10.1039/c1gc15350a

Geboers JA, Van de Vyver S, Ooms R, de Beeck BO, Jacobs PA, Sels BF (2011b) Chemocatalytic conversion of cellulose: opportunities, advances and pitfalls. Catal Sci Technol 1(5):714–726. https://doi.org/10.1039/c1cy00093d

Hanson SK, Baker RT, Gordon JC, Scott BL, Sutton AD, Thorn DL (2009) Aerobic oxidation of pinacol by vanadium(V) dipicolinate complexes: evidence for reduction to vanadium(III). J Am Chem Soc 131(2):428–429. https://doi.org/10.1021/ja807522n

He JY, Zhao C, Lercher JA (2012) Ni-catalyzed cleavage of aryl ethers in the aqueous phase. J Am Chem Soc 134(51):20768–20775. https://doi.org/10.1021/ja309915e

Hu L, Luo Y, Cai B, Li J, Tong D, Hu C (2014) The degradation of the lignin in Phyllostachys heterocycla cv. pubescens in an ethanol solvothermal system. Green Chem 16(6):3107–3116. https://doi.org/10.1039/c3gc42489h

Huang X, Koranyi TI, Boot MD, Hensen EJ (2014) Catalytic depolymerization of lignin in supercritical ethanol. Chemsuschem 7(8):2276–2288. https://doi.org/10.1002/cssc.201402094

Huber GW, Iborra S, Corma A (2006) Synthesis of transportation fuels from biomass: chemistry, catalysts, and engineering. Chem Rev 106(9):4044–4098. https://doi.org/10.1021/cr068360d

Jastrzebski R, Constant S, Lancefield CS, Westwood NJ, Weckhuysen BM, Bruijnincx PCA (2016) Tandem catalytic depolymerization of lignin by water-tolerant lewis acids and rhodium complexes. Chemsuschem 9(16):2074–2079. https://doi.org/10.1002/cssc.201600683

Jiang Z, Yi J, Li J, He T, Hu C (2015) Promoting effect of sodium chloride on the solubilization and depolymerization of cellulose from raw biomass materials in water. Chemsuschem 8(11):1901–1907. https://doi.org/10.1002/cssc.201500158

Jiang Z, Zhang H, He T, Lv X, Yi J, Li J, Hu C (2016) Understanding the cleavage of inter- and intramolecular linkages in corncob residue for utilization of lignin to produce monophenols. Green Chem 18(14):4109–4115. https://doi.org/10.1039/c6gc00798h

Jiang ZC, Zhao PP, Hu CW (2018) Controlling the cleavage of the inter- and intra-molecular linkages in lignocellulosic biomass for further biorefining: a review. Bioresour

Technol 256:466–477. https://doi.org/10.1016/j.biortech.2018.02.061

Kadokawa JI, Kaneko Y, Tagaya H, Chiba K (2001) Synthesis of an amylose–polymer inclusion complex by enzymatic polymerization of glucose 1-phosphate catalyzed by phosphorylase enzyme in the presence of polyTHF: a new method for synthesis of polymer–polymer inclusion complexes. Chem Commun 5:449–450

Kelley P, Lin SB, Edouard G, Day MW, Agapie T (2012) Nickel-mediated hydrogenolysis of c-o bonds of aryl ethers: what is the source of the hydrogen? J Am Chem Soc 134(12):5480–5483. https://doi.org/10.1021/ja300326t

Kondo T, Sawatari C (1996) A Fourier transform infra-red spectroscopic analysis of the character of hydrogen bonds in amorphous cellulose. Polymer 37(3):393–399. https://doi.org/10.1016/0032-3861(96)82908-9

Lahive CW, Deuss PJ, Lancefield CS, Sun ZH, Cordes DB, Young CM, Tran F, Slawin AMZ, de Vries JG, Kamer PCJ, Westwood NJ, Barta K (2016) Advanced model compounds for understanding acid-catalyzed lignin depolymerization: identification of renewable aromatics and a lignin-derived solvent. J Am Chem Soc 138(28):8900–8911. https://doi.org/10.1021/jacs.6b04144

Liang GF, Wu CY, He LM, Ming J, Cheng HY, Zhuo LH, Zhao FY (2011) Selective conversion of concentrated microcrystalline cellulose to isosorbide over Ru/C catalyst. Green Chem 13(4):839–842. https://doi.org/10.1039/c1gc15098g

Liao YH, Liu QY, Wang TJ, Long JX, Ma LL, Zhang Q (2014) Zirconium phosphate combined with Ru/C as a highly efficient catalyst for the direct transformation of cellulose to C-6 alditols. Green Chem 16(6):3305–3312. https://doi.org/10.1039/c3gc42444h

Liu Y, Chen L, Wang T, Zhang Q, Wang C, Yan J, Ma L (2015) One-pot catalytic conversion of raw lignocellulosic biomass into gasoline alkanes and chemicals over LiTaMoO6and Ru/C in aqueous phosphoric acid. Acs Sustain Chem Eng 3(8):1745–1755. https://doi.org/10.1021/acssuschemeng.5b00256

Lohr TL, Li Z, Marks TJ (2015) Selective ether/ester C–O cleavage of an acetylated lignin model via tandem catalysis. Acs Catal 5(11):7004–7007. https://doi.org/10.1021/acscatal.5b01972

Long J, Xu Y, Wang T, Yuan Z, Shu R, Zhang Q, Ma L (2015) Efficient base-catalyzed decomposition and in situ hydrogenolysis process for lignin depolymerization and char elimination. Appl Energy 141:70–79. https://doi.org/10.1016/j.apenergy.2014.12.025

Luterbacher JS, Azarpira A, Motagamwala AH, Lu FC, Ralph J, Dumesic JA (2015) Lignin monomer production integrated into the gamma-valerolactone sugar platform. Energy Environ Sci 8(9):2657–2663. https://doi.org/10.1039/c5ee01322d

Lv W, Si Z, Tian ZP, Wang CG, Zhang Q, Xu Y, Wang TJ, Ma LL (2017) Synergistic effect of EtOAc/H2O biphasic solvent and Ru/C catalyst for cornstalk hydrolysis residue depolymerization. Acs Sustain Chem Eng 5(4):2981–2993. https://doi.org/10.1021/acssuschemeng.6b02535

Marcus Y (1993) The properties of organic liquids that are relevant to their use as solvating solvents. Chem Soc Rev 22(6):409–416. https://doi.org/10.1039/cs9932200409

Min DY, Yang CM, Chiang V, Jameel H, Chang HM (2014) The influence of lignin-carbohydrate complexes on the cellulase-mediated saccharification II: transgenic hybrid poplars (*Populus nigra* L. and *Populus maximowiczii* A.). Fuel 116:56–62. https://doi.org/10.1016/j.fuel.2013.07.046

Miyagawa Y, Kamitakahara H, Takano T (2013) Fractionation and characterization of lignin-carbohydrate complexes (LCCs) of Eucalyptus globulus in residues left after MWL isolation. Part II: analyses of xylan-lignin fraction (X-L). Holzforschung 67(6):629–642. https://doi.org/10.1515/hf-2012-0148

Molinari V, Giordano C, Antonietti M, Esposito D (2014) Titanium nitride-nickel nanocomposite as heterogeneous catalyst for the hydrogenolysis of aryl ethers. J Am Chem Soc 136(5):1758–1761. https://doi.org/10.1021/ja4119412

Oh SY, Yoo DI, Shin Y, Kim HC, Kim HY, Chung YS, Park WH, Youk JH (2005) Crystalline structure analysis of cellulose treated with sodium hydroxide and carbon dioxide by means of X-ray diffraction and FTIR spectroscopy. Carbohydr Res 340(15):2376–2391. https://doi.org/10.1016/j.carres.2005.08.007

Onwudili JA, Williams PT (2014) Catalytic depolymerization of alkali lignin in subcritical water: influence of formic acid and Pd/C catalyst on the yields of liquid monomeric aromatic products. Green Chem 16(11):4740–4748. https://doi.org/10.1039/c4gc00854e

Op de Beeck B, Geboers J, Van de Vyver S, Van Lishout J, Snelders J, Huijgen WJJ, Courtin CM, Jacobs PA, Sels BF (2013) Conversion of (Ligno) cellulose feeds to isosorbide with heteropoly acids and Ru on carbon. Chemsuschem 6(1):199–208. https://doi.org/10.1002/cssc.201200610

Pandey MP, Kim CS (2011) Lignin depolymerization and conversion: a review of thermochemical methods. Chem Eng Technol 34(1):29–41. https://doi.org/10.1002/ceat.201000270

Payne CM, Resch MG, Chen LQ, Crowley MF, Himmel ME, Taylor LE, Sandgren M, Stahlberg J, Stals I, Tan ZP, Beckham GT (2013) Glycosylated linkers in multimodular lignocellulose-degrading enzymes dynamically bind to cellulose. Proc Natl Acad Sci USA 110(36):14646–14651. https://doi.org/10.1073/pnas.1309106110

Pouteau C, Cathala B, Dole P, Kurek B, Monties B (2005) Structural modification of Kraft lignin after acid treatment: characterisation of the apolar extracts and influence on the antioxidant properties in polypropylene. Ind Crops Prod 21(1):101–108. https://doi.org/10.1016/j.indcrop.2004.01.003

Ragauskas AJ, Beckham GT, Biddy MJ, Chandra R, Chen F, Davis MF, Davison BH, Dixon RA, Gilna P, Keller M, Langan P, Naskar AK, Saddler JN, Tschaplinski TJ, Tuskan GA, Wyman CE (2014) Lignin valorization: improving lignin processing in the biorefinery. Science 344(6185):709–719. https://doi.org/10.1126/science.1246843

Resch MG, Donohoe BS, Baker JO, Decker SR, Bayer EA, Beckham GT, Himmel ME (2013) Fungal cellulases and complexed cellulosomal enzymes exhibit synergistic mechanisms in cellulose deconstruction. Energy Environ Sci 6(6):1858–1867. https://doi.org/10.1039/c3ee00019b

Richards NJ, Williams DG (1970) Complex formation between aqueous zinc chloride and cellulose-related

D-glucopyranosides. Carbohyd Res 12(3):409–420. https://doi.org/10.1016/S0008-6215(00)80621-7

Roman-Leshkov Y, Barrett CJ, Liu ZY, Dumesic JA (2007) Production of dimethylfuran for liquid fuels from biomass-derived carbohydrates. Nature 447(7147):U982–U985. https://doi.org/10.1038/nature05923

Rondeau P, Sers S, Jhurry D, Cadet F (2003) Sugar interaction with metals in aqueous solution: indirect determination from infrared and direct determination from nuclear magnetic resonance spectroscopy. Appl Spectrosc 57(4):466–472. https://doi.org/10.1366/00037020360626023

Ruppert AM, Weinberg K, Palkovits R (2012) Hydrogenolysis goes bio: from carbohydrates and sugar alcohols to platform chemicals. Angew Chem Int Ed 51(11):2564–2601. https://doi.org/10.1002/anie.201105125

Schwanninger M, Rodrigues JC, Pereira H, Hinterstoisser B (2004) Effects of short-time vibratory ball milling on the shape of FT-IR spectra of wood and cellulose. Vib Spectrosc 36(1):23–40. https://doi.org/10.1016/j.vibspec.2004.02.003

Sen S, Martin JD, Argyropoulos DS (2013) Review of cellulose non-derivatizing solvent interactions with emphasis on activity in inorganic molten salt hydrates. Acs Sustain Chem Eng 1(8):858–870. https://doi.org/10.1021/sc400085a

Sergeev AG, Webb JD, Hartwig JF (2012) A heterogeneous nickel catalyst for the hydrogenolysis of aryl ethers without arene hydrogenation. J Am Chem Soc 134(50):20226–20229. https://doi.org/10.1021/ja3085912

Shu R, Long J, Yuan Z, Zhang Q, Wang T, Wang C, Ma L (2015) Efficient and product-controlled depolymerization of lignin oriented by metal chloride cooperated with Pd/C. Bioresour Technol 179:84–90. https://doi.org/10.1016/j.biortech.2014.12.021

Shuai L, Luterbacher J (2016) Organic solvent effects in biomass conversion reactions. Chemsuschem 9(2):133–155. https://doi.org/10.1002/cssc.201501148

Shuai L, Amiri MT, Questell-Santiago YM, Heroguel F, Li YD, Kim H, Meilan R, Chapple C, Ralph J, Luterbacher JS (2016) Formaldehyde stabilization facilitates lignin monomer production during biomass depolymerization. Science 354(6310):329–333. https://doi.org/10.1126/science.aaf7810

Sluiter A, Hames B, Ruiz R, Scarlata C, Sluiter J, Templeton D, Crocker D (2008) Determination of structural carbohydrates and lignin in biomass: laboratory analytical procedure (LAP). NREL Transform Energy 1617:1–6

Somerville C, Youngs H, Taylor C, Davis SC, Long SP (2010) Feedstocks for lignocellulosic biofuels. Science 329(5993):790–792. https://doi.org/10.1126/science.1189268

Sturgeon MR, O'Brien MH, Ciesielski PN, Katahira R, Kruger JS, Chmely SC, Hamlin J, Lawrence K, Hunsinger GB, Foust TD, Baldwin RM, Biddy MJ, Beckham GT (2014) Lignin depolymerisation by nickel supported layered-double hydroxide catalysts. Green Chem 16(2):824–835. https://doi.org/10.1039/c3gc42138d

Van den Bosch S, Schutyser W, Koelewijn SF, Renders T, Courtin CM, Sels BF (2015a) Tuning the lignin oil OH-content with Ru and Pd catalysts during lignin hydrogenolysis on birch wood. Chem Commun 51(67):13158–13161. https://doi.org/10.1039/c5cc04025f

Van den Bosch S, Schutyser W, Vanholme R, Driessen T, Koelewijn SF, Renders T, De Meester B, Huijgen WJJ, Dehaen W, Courtin CM, Lagrain B, Boerjan W, Sels BF (2015b) Reductive lignocellulose fractionation into soluble lignin-derived phenolic monomers and dimers and processable carbohydrate pulps. Energy Environ Sci 8(6):1748–1763. https://doi.org/10.1039/c5ee00204d

Vispute TP, Zhang HY, Sanna A, Xiao R, Huber GW (2010) Renewable chemical commodity feedstocks from integrated catalytic processing of pyrolysis oils. Science 330(6008):1222–1227. https://doi.org/10.1126/science.1194218

Vitz J, Erdmenger T, Haensch C, Schubert US (2009) Extended dissolution studies of cellulose in imidazolium based ionic liquids. Green Chem 11(3):417–424. https://doi.org/10.1039/b818061j

vom Stein T, den Hartog T, Buendia J, Stoychev S, Mottweiler J, Bolm C, Klankermayer J, Leitner W (2015) Ruthenium-catalyzed C–C bond cleavage in lignin model substrates. Angew Chem Int Ed 54(20):5859–5863. https://doi.org/10.1002/anie.201410620

Wang H, Gurau G, Rogers RD (2012) Ionic liquid processing of cellulose. Chem Soc Rev 41(4):1519–1537. https://doi.org/10.1039/c2cs15311d

Xie YM, Yasuda S, Wu H, Liu HB (2000) Analysis of the structure of lignin—carbohydrate complexes by the specific C-13 tracer method. J Wood Sci 46(2):130–136. https://doi.org/10.1007/Bf00777359

Xu Q, Chen LF (1999) Ultraviolet spectra and structure of zinc–cellulose complexes in zinc chloride solution. J Appl Polym Sci 71(9):1441–1446

Xu CP, Arancon RAD, Labidi J, Luque R (2014) Lignin depolymerisation strategies: towards valuable chemicals and fuels. Chem Soc Rev 43(22):7485–7500. https://doi.org/10.1039/c4cs00235k

Xue ZM, Zhao XH, Sun RC, Mu TC (2016) Biomass-derived gamma-valerolactone-based solvent systems for highly efficient dissolution of various lignins: dissolution behavior and mechanism study. Acs Sustain Chem Eng 4(7):3864–3870. https://doi.org/10.1021/acssuschemeng.6b00639

Yu Y, Liu DW, Wu HW (2014) Formation and characteristics of reaction intermediates from the fast pyrolysis of NaCl- and MgCl2-loaded celluloses. Energy Fuel 28(1):245–253. https://doi.org/10.1021/ef401483u

Zakzeski J, Bruijnincx PCA, Jongerius AL, Weckhuysen BM (2010) The catalytic valorization of lignin for the production of renewable chemicals. Chem Rev 110(6):3552–3599. https://doi.org/10.1021/cr900354u

Zhang XQ, Chen MJ, Wang HH, Liu CF, Zhang AP, Sun RC (2015) Characterization of xylan-graft-polycaprolactone copolymers prepared in ionic liquid. Ind Eng Chem Res 54(24):6282–6290. https://doi.org/10.1021/acs.iecr.5b01323

Zhang H, Liu XD, Li JM, Jiang ZC, Hu CW (2018) Performances of several solvents on the cleavage of inter- and intramolecular linkages of lignin in corncob residue. Chemsuschem 11(9):1494–1504. https://doi.org/10.1002/cssc.201800309

Zhao C, Kou Y, Lemonidou AA, Li XB, Lercher JA (2009) Highly selective catalytic conversion of phenolic bio-oil to alkanes. Angew Chem Int Ed 48(22):3987–3990. https://doi.org/10.1002/anie.200900404